iScience

CellPress
OPEN ACCESS

Article

Time- and sex-dependent delayed effects of acute radiation exposure manifest via miRNA dysregulation

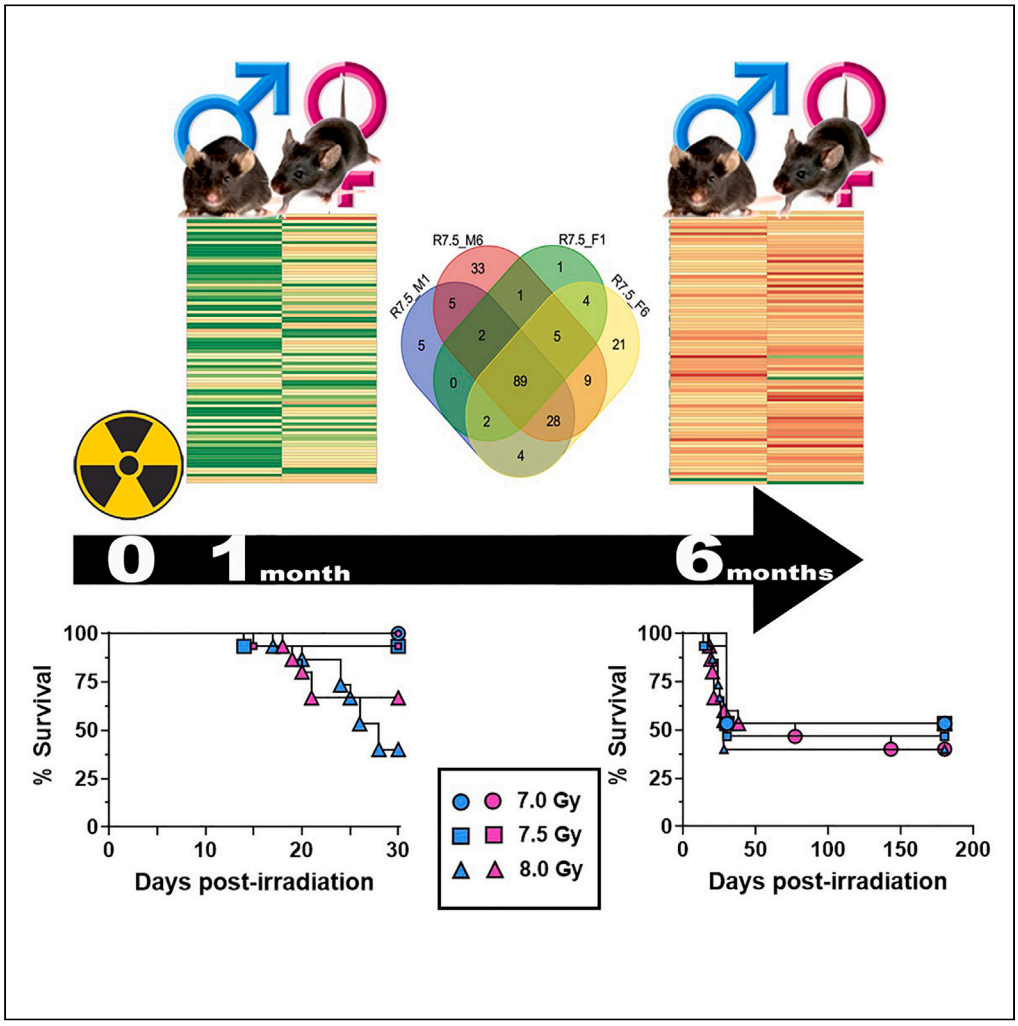

Gregory P. Holmes-Hampton, Dharmendra Kumar Soni, Vidya P. Kumar, Shukla Biswas, Kefale Wuddie, Roopa Biswas, Sanchita P. Ghosh

roopa.biswas@usuhs.edu (R.B.)
sanchita.ghosh@usuhs.edu (S.P.G.)

Highlights

Sex differences' impact on delayed effects of acute radiation (DEAREs) is unclear

DEARE alters miRNA and HOTAIR pathway in time- and sex-dependent ways

Disease and cellular functions differ in male/female mice

Findings reveal molecular basis of age/sex differences in DEARE

Holmes-Hampton et al., iScience 27, 108867
February 16, 2024
https://doi.org/10.1016/j.isci.2024.108867

iScience

CellPress
OPEN ACCESS

Article

Time- and sex-dependent delayed effects of acute radiation exposure manifest via miRNA dysregulation

Gregory P. Holmes-Hampton,[1,3] Dharmendra Kumar Soni,[2,3] Vidya P. Kumar,[1] Shukla Biswas,[1] Kefale Wuddie,[1] Roopa Biswas,[2,*] and Sanchita P. Ghosh[1,4,*]

SUMMARY

The detrimental effects of high-dose ionizing radiation on human health are well-known, but the influence of sex differences on the delayed effects of acute radiation exposure (DEARE) remains unclear. Here, we conducted six-month animal experiments using escalating radiation doses (7–9 Gy) on male and female C57BL/6 mice. The results show that female mice exhibited greater resistance to radiation, showing increased survival at six months post-total body irradiation. LD50/30 (lethal dose expected to cause 50% lethality in 30 days) for female mice is 8.08 Gy, while for male mice it is 7.76 Gy. DEARE causes time- and sex-dependent dysregulation of microRNA expression, processing enzymes, and the HOTAIR regulatory pathway. Differential regulation of molecular patterns associated with growth, development, apoptosis, and cancer is also observed in male and female mice. These findings shed light on the molecular basis of age and sex differences in DEARE response and emphasize the importance of personalized medicine for mitigating radiation-induced injuries and diseases.

INTRODUCTION

The current state of global conflict, military tensions, radiation disasters, and rise in prevalence of radiotherapy brings about the risk of exposure to radiation through intentional or accidental means worldwide.[1–4] High doses of ionizing radiation can cause tissue damage and harm to vital organs, leading to hematopoietic acute radiation syndrome (H-ARS), and gastrointestinal acute radiation syndrome (GI-ARS), with high morbidity and mortality rates.[5] For exposed individuals who survive acute radiation exposure or are exposed to sub-lethal doses, it is still likely they will experience delayed effects of acute radiation exposure (DEARE), which can include chronic illnesses that affect multiple organs such as lungs, liver, kidney, brain, and heart.[6–8] This may result in long-term health problems like cancer, cardiovascular disease, and hereditary problems. Thus, it is necessary to comprehend the long-term health effects of DEARE, late morbidity and mortality.

Previous work has suggested that DEARE will manifest with different levels of severity depending on radiation dose, exposure duration, and radiation quality, compounded by demographic variables such as age, sex, and health of the exposed individual.[9–11] Among these factors, assessment of sex differences in sensitivity and long-term response to radiation exposure is not well understood. The International Commission on Radiological Protection (ICRP) has made their recommendations based on the average of the whole population instead of different radiosensitivity data from subgroups and also recommends the same protection standards for both men and women.[12–14] However, the National Academy of Sciences (NAS) 2006 report on biological effects of ionizing radiation (BEIR VII) demonstrated that women may be more likely to suffer and die from cancers caused by ionizing radiation than men exposed to the same amount of radiation.[15] Also, the United Nations Scientific Committee on the Effects of Atomic Radiation (UNSCEAR) believes that compared to men women experience a 1.5 times higher absolute and relative risk of developing solid cancers.[16] Similarly, the Nuclear Information and Resource Service (NIRS) also showed that radiation has a greater impact on women, with 50% more cancer cases and fatalities reported among women than men for the same radiation exposure.[17]

Research in animals has suggested that exposure to ionizing radiation has different impacts on males and females, as evidenced by the different gene/protein expression profiles in various tissues of male and female mice exposed to both acute and chronic low-dose whole-body irradiation.[18–23] These findings point to the existence of numerous pathways that are affected differently depending on sex. Likewise, DEARE studies also disclosed different effects on male and female mice.[24–26] This implies that sex-related factors may play a role in the long-term response to radiation exposure. Nonetheless, the associated cellular and molecular mechanisms for these variations in sensitivity and long-term response to radiation exposure remain unclear. Gaining a deeper insight into the sex-specific mechanisms that contribute to the

[1]Armed Forces Radiobiology Research Institute, Uniformed Services University of the Health Sciences, Bethesda, MD 20889, USA
[2]Department of Anatomy, Physiology and Genetics, School of Medicine, Uniformed Services University of the Health Sciences, Bethesda, MD 21045, USA
[3]These authors contributed equally
[4]Lead contact
*Correspondence: roopa.biswas@usuhs.edu (R.B.), sanchita.ghosh@usuhs.edu (S.P.G.)
https://doi.org/10.1016/j.isci.2024.108867

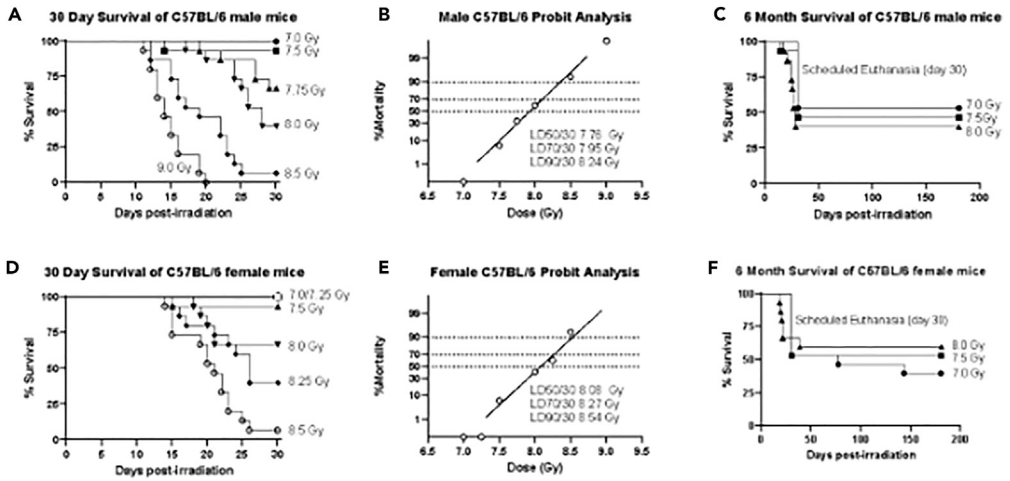

Figure 1. Effect of various doses of radiation on mouse survival

Kaplan-Meier survival curves depict the 30-day post-TBI survival of (A) male and (D) female C57BL/6 mice exposed to various radiation doses. Probit analysis of the 30-day post-TBI survival curves for (B) male and (E) female mice indicates the LD50/30, LD70/30, and LD90/30 values. Kaplan-Meier curves show the 6-month post-TBI survival of (C) male and (F) female mouse groups exposed to three radiation doses (7.0, 7.5, and 8.0 Gy).

varying degrees of DEARE is key to formulating medical interventions, assessing the efficacy of treatments, and developing radiation safety guidelines and potential therapies. Studies have revealed that microRNAs (miRNAs, miRs), small, single-stranded noncoding RNAs (~19–21 nucleotides), are important regulators of nearly every cellular and molecular process.[27–29] They do this in a sequence-specific manner at the post-transcriptional level by either degrading the target messenger RNA (mRNA) and/or inhibiting its translation.

In this study, we performed animal experiments for a period of six months with six increasing doses of radiation (7–9 Gy, ^{60}Co γ-radiation) in male and female C57BL/6 mice to understand the sex differences in DEARE. Further, we examined global changes in the expression of miRNAs and associated pathways in the serum samples of male and female mice that had been irradiated and compared to non-irradiated mice, at two time points: one and six months post-total body irradiation (TBI). Our results indicate that female mice are relatively radioresistant than male mice and at 6 months post-TBI (7.5 and 8 Gy) female mice have increased survival and lethal dose expected to cause 50% lethality in 30 days (LD50/30) compared to male mice. Further analysis demonstrates that DEARE affects in a time- and sex-dependent manner through dysregulation of miRNA expression and biogenesis and provides new insights into the DEARE-mediated molecular and cellular mechanisms. Collectively, these data along with earlier studies point toward personalized medicine for the prevention of radiation-induced injuries and diseases.

RESULTS

Sex-specific differences in radioresistance over 6 months post-TBI

Mice (n = 15 per group) were exposed to different radiation doses to assess 30-day lethality and gender-based differences. Long-term survival was monitored for up to 6 months post-TBI. For male mice, survival rates at day 30 were 100% (7.0 Gy), 93% (7.5 Gy), 67% (7.75 Gy), 40% (8.0 Gy), 7% (8.5 Gy), and 0% (9.0 Gy) (Figure 1A). LD50/30, LD70/30, and LD90/30 were determined as 7.76 Gy, 7.95 Gy, and 8.24 Gy, respectively (Figure 1B). No further mortalities occurred beyond day 30 for doses of 7.0, 7.5, and 8.0 Gy (Figure 1C). For female mice, day 30 survival rates were 100% (7.0 Gy), 100% (7.25 Gy), 97% (7.5 Gy), 67% (8.0 Gy), 40% (8.25 Gy), and 7% (8.5 Gy) (Figure 1D). LD50/30, LD70/30, and LD90/30 were determined as 8.08 Gy, 8.27 Gy, and 8.54 Gy, respectively (Figure 1E). Notably, a ~13% mortality was observed at 6 months post-TBI for the lowest dose (7.0 Gy), which initially showed no mortality (Figure 1F). Overall, these results indicate that female mice exhibit greater radiation resistance than male mice, as evidenced by higher 6-month post-TBI survival rates at doses of 7.5 and 8 Gy and a higher LD50/30 value of 8.08 Gy for female mice compared to 7.76 Gy for male mice.

Body weight (BW) changes in mice over 6 months post-TBI

Surviving male and female mice exposed to radiation doses of 7.0, 7.5, and 8.0 Gy along with age-matched non-irradiated animals were monitored for six months post-TBI. BWs were recorded monthly. A steady increase in BW of male mice was observed over the 6-month post-TBI period (Figure 2A, left; Table S1). These results imply that the animals at the highest dose gained the least weight over the 6-month post-TBI period. However, it is also worth noting that the animals from the 8.0 Gy radiation dose also had the highest starting BW. A similar trend of increased BW was observed for the female mice over the 6-month post-TBI observation period (Figure 2A, right; Table S1). For animals in this age range (~12 weeks at the time of irradiation) the changes in BW observed here are typical. In summary, there were no significant

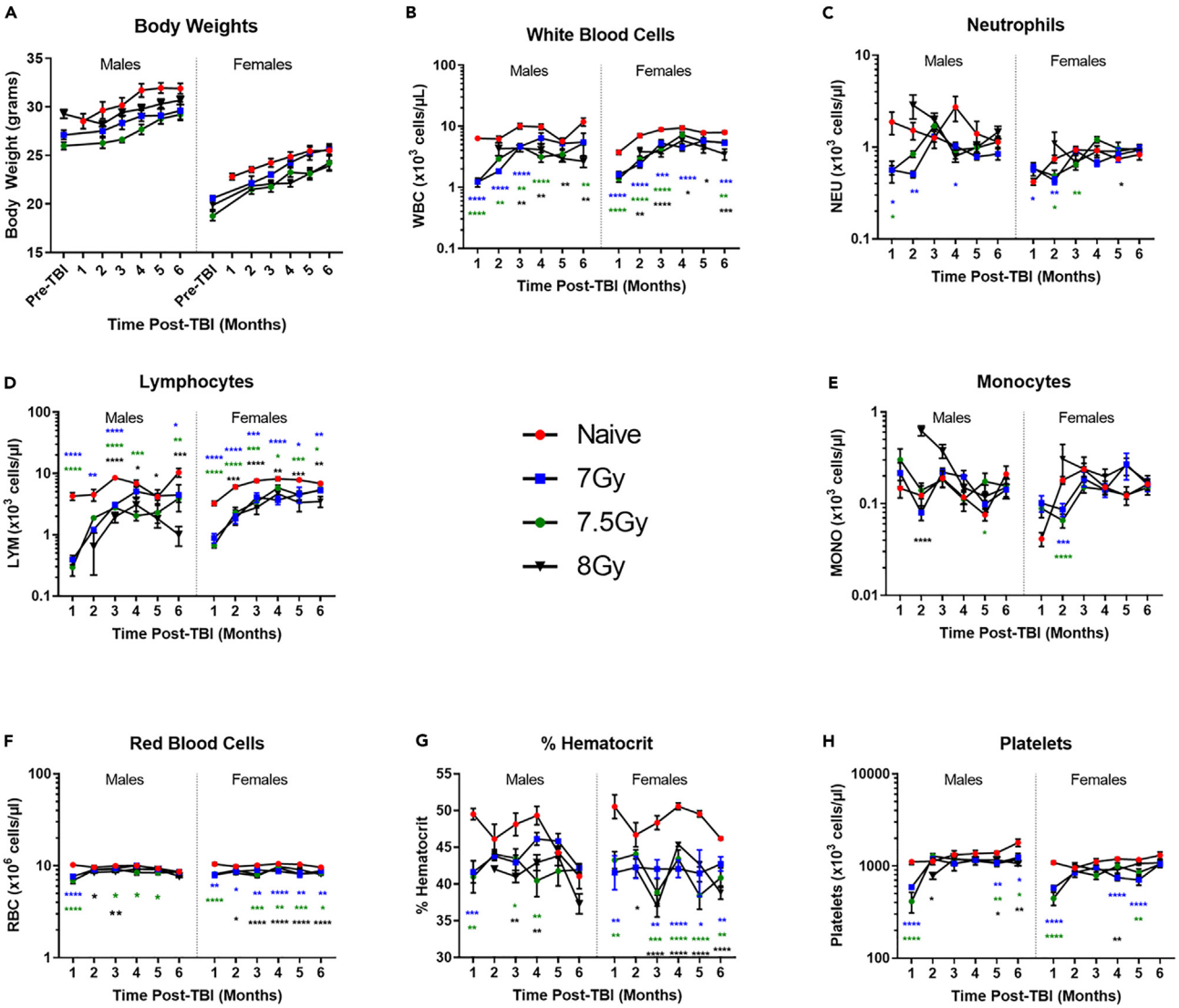

Figure 2. Body weight and peripheral blood cell counts

Mice exposed to doses of 7.0, 7.5, or 8.0 Gy were analyzed for up to 6 months post-TBI.

(A) Body weights of male (left) and female (right) mice post-TBI are shown.

(B–H) The graphs depict WBC, NEU, LYM, MONO, RBC, %HCT, and PLT counts in both the control non-irradiated (naive) and irradiated male (left) and female (right) mouse groups. The center legend is common to all graphs. Data are presented as means ± standard error of mean (SEM). Significance compared to naive group is indicated as follows: *p < 0.05, **p < 0.01, ***p < 0.001, ****p < 0.0001. The color of the asterisk corresponds to the group. N = 5–8 mice/group/sex.

sex-specific differences in BW changes following TBI, as both male and female mice showed a similar increasing trend in BW over the six-month period. Therefore, DEARE did not appear to have a significant sex-specific impact on BW.

Hematological changes in mice over 6 months post-TBI

Blood samples (~20 μL) were collected (via the submandibular vein) monthly from surviving male and female mice exposed to 7.0, 7.5, and 8.0 Gy, along with age-matched non-irradiated animals, for complete blood count (CBC) analysis. Over a 6-month period following exposure to different radiation doses, both male and female mice exhibited similar hematological changes (Figures 2B–2H; Table S2). There were no significant sex-specific differences in blood cell parameters, including neutrophils (NEUs), lymphocytes (LYMs), monocytes (MONOs), red blood cells (RBCs), hematocrit (HCT), and platelets (PLTs), except for white blood cells (WBCs) count. Male mice had significantly reduced WBC counts compared to naive mice as well as the normal defined levels for this strain.[30] However, the WBC counts were restored to near-normal levels by month 4 for male mice exposed to the lowest radiation dose (7.0 Gy). Interestingly, the female mice had significantly reduced WBC

counts for all radiation doses (7.0 Gy, 7.5 Gy, and 8.0 Gy). These findings suggest that radiation-induced alterations in blood cell parameters do not appear to differ between male and female mice, indicating that DEARE does not have a significant sex-specific impact on these parameters.

Impact of TBI on total bone marrow and megakaryocyte counts in mice

We quantified bone marrow colony-forming units (CFUs) using bone marrow isolated from the femurs of animals euthanized at the 1-month and 6-month post-TBI time points (Figure S1A). At the 1-month post-TBI time point, samples were obtained from both male and female mice irradiated at 7.0 and 7.5 Gy. At the 6-month post-TBI time points, samples were obtained from both male and female mice irradiated at 7.0 and 7.5 Gy, and from female mice only at 8.0 Gy. Due to insufficient surviving animals in the 8.0 Gy group, we were unable to collect samples from these animals at the one-month post-TBI time point and from the male mice at the 6-month post-TBI time point. Bone marrow CFUs were classified as burst-forming unit-erythroid (BFU-E), granulocyte, erythrocyte, monocyte, megakaryocyte colony-forming units (CFU-GEMM), or granulocyte monocyte colony-forming units (CFU-GM). We quantified each lineage as well as the total number of CFUs.

Over a six-month period following TBI, male and female mice showed similar trends in bone marrow CFU and megakaryocyte counts. TBI resulted in decreased CFU counts, specifically BFU-E, granulocyte, erythrocyte, monocyte, and CFU-GEMM colonies, in both male and female mice. There were no significant differences between irradiated male and female mice groups. Additionally, megakaryocyte numbers in the bone marrow sternum were not significantly different between male and female mice, except for a specific comparison for female mice at one-month post-TBI (naive vs. 7.5 Gy) and for male mice at six-month post-TBI (naive vs. 8 Gy) (Figure S1B). These findings suggest that TBI does not have a significant sex-specific impact on bone marrow progenitor cells and megakaryocytes over the six-month period.

Impact of TBI on histopathological changes in different organs tissue

One-month time point

Tissue samples were collected at the 1-month post-TBI (naive, 7.0, 7.5, and 8 Gy) stage and evaluated by a board-certified pathologist. Male mice had minimal lesions at the 1-month post-TBI time point. However, liver tissue from the male mice exposed to the highest radiation dose (8 Gy) showed a low number of foamy histiocytes within the alveolar septa (Table 1). This condition was noted as minimal to mild and considered insignificant. On the other hand, the liver tissues isolated from male mice exposed to the two lower doses, 7.0 Gy and 7.5 Gy, had small multifocal and random aggregates of mononuclear leukocyte infiltrates, with fewer neutrophils. Similar lesion is often seen in aging mice. Small foci of myocyte degeneration were found in the heart tissues of male mice exposed to TBI. Additionally, two mice from the 7.5 Gy group did not survive (Figure 3A). The possibility of radiation being the cause of these lesions could not be excluded. Furthermore, kidney tissue from male mice exposed to TBI exhibited focally extensive fibrosis centered on an arcuate artery at the corticomedullary boundary (Figure 3B). Fibrosis is a result of cytokine release, which may be a consequence of irradiation.

The lung tissues of female mice showed mild aggregation of mononuclear cellular infiltrates composed of lymphocytes, plasma cells, and fewer histiocytes situated randomly within the interstitium. In the liver tissues (all groups including naive), there were small multifocal and random aggregates of lymphocytes and plasma cells, with fewer neutrophils (Figure 3C). Since this was observed in naive animals as well, it is unlikely to be related to irradiation. No significant lesions were observed in the female mouse heart tissues; however, kidney tissues had histological features consistent with focally extensive wedge fibrosis radiating out from the corticomedullary junction to the cortical surface.

Six-month time point

Samples were also analyzed from animals at 6 months post-TBI which were exposed to various radiation doses (naive, 7.0, 7.5, and 8.0 Gy). Lesions were noted in the lung tissues of male mice (7.5 Gy and 8.0 Gy). Occasional and random small aggregates of mononuclear cellular infiltrates, composed of lymphocytes, plasma cells, and fewer histiocytes were observed, which may not be caused exclusively by irradiation. Small multifocal and random aggregates of mononuclear leukocytes, with fewer neutrophils, were observed in the liver tissues obtained from male mice including the naive group. These lesions are common in aging animals and do not seem to be induced by exposure to radiation. No significant histologic changes were observed in the heart tissues of male mice. Several lesions were observed in the mouse kidney tissues obtained from male mice, including extensive fibrosis, moderate-sized mononuclear leukocyte aggregates, and smaller aggregates of mononuclear leukocyte infiltrates in the cortex (Table 1 with details).

Lung tissues isolated from female mice showed multifocal to coalescing lymphoma affecting more than half of the lung tissue section (Figure 3D). Liver tissues obtained from female mice had mild- to moderate-sized multifocal and random aggregates of lymphocytes and plasma cells, with fewer neutrophils affecting many liver sections from all subsets (7.0, 7.5, and 8.0 Gy TBI, naive subsets). There were no significant histologic changes in the heart tissues of these female mice. The kidney tissues obtained from female mice had segmental glomerular sclerosis affecting glomerular tufts.

Together, these results indicate that within all irradiated groups (7.0, 7.5, and 8.0 Gy), including both male and female mice, and both 1 and 6 months post-TBI groups, random animals demonstrate abnormalities in the liver, kidney, heart, and lungs.

Expression of miRNAs varies in a time- and sex-dependent manner

To explore whether in response to DEARE the expression of miRNAs is distinctively altered in male and female mice, we performed a comprehensive analysis of miRNA expression profiles from the serum of the irradiated male (n = 12) and female (n = 12) mouse groups in comparison

Table 1. Histopathological changes in irradiated mice at 1 and 6 months post-TBI

		Male mice (post-TBI)		Female mice (post-TBI)	
Histopathological changes	Radiation doses (Gy)	1 month (n = 5/group)	6-month (n = 5/group	1-month (n = 5/group)	6-month (n = 5/group)
Lung	7, 7.5, 8	minimal lesions	minimal to mild and considered insignificant; however, lesions were noted in the lungs of a single male mice at 7.5 Gy and 8.0 Gy. Occasional and random small aggregates of mononuclear cellular infiltrates composed of lymphocytes, plasma cells, and fewer histiocytes were observed, which may not be caused exclusively by irradiation	minimal lesions; however, one of the mice lung tissue from the 7.5 Gy group showed mild aggregation of mononuclear cellular infiltrates composed of lymphocytes, plasma cells, and fewer histiocytes situated randomly within interstitium, which was rated mild (n = 1)	minimal lesions; however, a female mouse from the 7.0 Gy group showed multifocal to coalescing lymphoma that affects more than half of the lung tissue section (n = 1)
Liver	7	minimal to mild and considered insignificant; however, small multifocal and random aggregates of mononuclear leukocyte infiltrates were observed, with fewer neutrophils (n = 1)	small multifocal and random aggregates of mononuclear leukocytes, with fewer neutrophils observed in the liver of several animals including naive (n = 4), 7.0 Gy group (n = 3), 7.5 Gy group (n = 1), and 8.0 Gy group (n = 2)	small multifocal and random aggregates of lymphocytes and plasma cells, with fewer neutrophils, considered insignificant since this was also observed in the naive animals	Mild- to moderate-sized multifocal and random aggregates of lymphocytes, plasma cells, with fewer neutrophils affecting many liver sections
	7.5	small multifocal and random aggregates of mononuclear leukocyte infiltrates, with fewer neutrophils (n = 5)			
	8	minimal to mild and considered insignificant; however, a low number of foamy histiocytes within the alveolar septa (n = 1)			
Heart	7, 7.5, 8	small foci of myocyte degeneration; however, two of the mice heart tissues from the 7.5 Gy group did not survive (n = 2)	no significant lesions	no significant lesions	no significant lesions

(*Continued on next page*)

Table 1. *Continued*

Histopathological changes	Radiation doses (Gy)	Male mice (post-TBI)		Female mice (post-TBI)	
		1 month (n = 5/group)	6-month (n = 5/group	1-month (n = 5/group)	6-month (n = 5/group)
Kidney	7, 7.5, 8	minimal lesions; however, one of the mice kidney tissue from the 7.0 Gy group was characterized by focally extensive fibrosis centered on an arcuate artery at the corticomedullary boundary (n = 1)	several lesions were observed in the mouse kidney, including extensive fibrosis (7.0 Gy group, n = 1), moderate-sized mononuclear leukocyte aggregates in the naive (n = 3), and smaller aggregates of mononuclear leukocyte infiltrates in the cortex of animals exposed to 7.0 Gy (n = 1) and 8.0 Gy (n = 2)	minimal lesions; however, one of the mice kidney tissue from the 7.5 Gy group shows histology features consistent with focally extensive wedge fibrosis that radiates out from the corticomedullary junction to the cortical surface (n = 1)	minimal lesions; however, segmental glomerular sclerosis was observed affecting glomerular tufts in 3 animals from 7.5 Gy group (n = 3) and a single animal from the 8.0 Gy group (n = 1)

Summaries of histopathological evaluations made by a board-certified pathologist of major organs including the lung, liver, heart, and kidney from male and female mice at 1 month and 6 months post-TBI are presented.

to non-irradiated animals (n = 12), respectively, at two time points, i.e., one and six months post-TBI. Subsequently, we compared these significantly altered serum miRNAs of the male group with those of the female group at both time points.

The analyses identified a total of 136 and 172 dysregulated miRNAs (≥1.5-fold) in the irradiated male mice groups at one month (R7.5_M1) and 6 months (R7.5_M6) post-TBI, respectively, compared to non-irradiated male groups (Figure 4A). Among the 136 miRNAs in the R7.5_M1 group, 131 were downregulated and 5 were upregulated. Similarly, among the 172 miRNAs in the R7.5_M6 group, 90 were downregulated and 82 were upregulated (Figure 4B). Likewise, in the irradiated female groups, a total of 104 and 162 dysregulated miRNAs (≥1.5-fold) were identified at one month (R7.5_F1) and 6 months (R7.5_F6) post-TBI, respectively, compared to non-irradiated female mice groups (Figure 4A). Among the 104 miRNAs in the R7.5_F1 group, 91 were downregulated and 13 were upregulated, whereas, among the 162 miRNAs in the R7.5_F6 group, 58 were downregulated and 104 were upregulated (Figure 4B). These outcomes reveal that, in response to DEARE, the downregulation of miRNAs is time and sex dependent, as at one-month post-TBI the total number of downregulated miRNAs was more in both male (R7.5_M1, 96.32%) and female (R7.5_F1, 87.50%) mice groups, which decreased at 6 months post-TBI in both male (R7.5_M6, 52.33%) and female (R7.5_F6, 35.80%) mice groups. Additionally, time- and sex-dependent upregulation of miRNAs was also observed, as the total number of upregulated miRNAs at one-month post-TBI in both male (R7.5_M1, 3.68%) and female (R7.5_F1, 12.50%) mice groups increased at 6 months post-TBI in both male (R7.5_M6, 47.67%) and female (R7.5_F6, 64.20%) mice.

Analyses also showed that 89 miRNAs were differentially expressed at both post-TBI time points and in both sexes (Figure 4C). However, as depicted in Figure 4D, most of the miRNAs (85) among these 89 miRNAs were downregulated in the R7.5_M1 group, which showed either less downregulation or upregulation in the R7.5_M6 group. Similarly, in the R7.5_F1 group, most of the miRNAs (80) among common miRNAs (89) were downregulated, which showed either less downregulation or upregulation in the R7.5_F6 group (Figure 4D). These results reveal that in response to DEARE the expression of miRNAs is altered in a time-dependent manner in murine serum.

Further, the comparative analyses of these 89 miRNAs in between sexes (R7.5_M1 and R7.5_F1 groups) showed that, among the downregulated miRNAs (85) in the R7.5_M1 group, 53 had less downregulation and 8 had upregulation in the R7.5_F1 group (Figure 4D). Similarly, comparative analyses between the R7.5_M6 and R7.5_F6 groups showed that among the downregulated miRNAs (52) in the R7.5_M6 group, 9 had less downregulation (9) and 27 had upregulation (27) in R7.5_F6 group (Figure 4D). These results imply that in response to DEARE the expression of miRNAs altered in a sex-dependent manner in murine serum.

Furthermore, we also found that 5, 33, 1, and 21 miRNAs were specifically expressed in the R7.5_M1, R7.5_M6, R7.5_F1, and R7.5_F6 groups, respectively (Figure 4C). The expression of specifically expressed miRNAs in the R7.5_M1, R7.5_M6, R7.5_F1, and R7.5_F6 groups is shown in Figures 4E–4H respectively. These results further imply that in response to DEARE the expression of miRNAs varies in murine serum in a time- and sex-dependent manner.

Regulation of the HOTAIR canonical pathway varies in a time- and sex-dependent manner

To identify the molecular mechanisms involved in DEARE, we performed *in silico* analysis of canonical pathways using the Ingenuity Pathway Analysis (IPA) program with the differentially expressed miRNAs of the irradiated male and female mice groups at both 1 and 6 months post-TBI. IPA analyses identified that the HOTAIR regulatory pathway was significantly activated (*Z* score ≥2) in the R7.5_M1 group

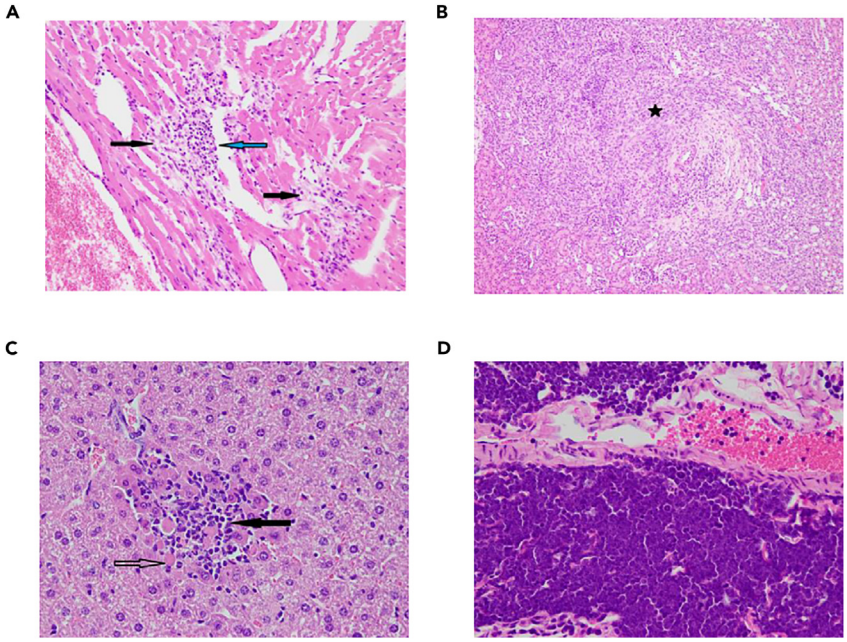

Figure 3. Histopathological changes

Mice exposed to doses of 7.0, 7.5, or 8.0 Gy were analyzed for up to 6 months post-TBI.

(A) Heart tissues from male mice irradiated with 7.5 Gy, 1-month post-TBI, show loss of cardiocytes, fibrosis (black arrow), and mononuclear leukocyte infiltrates (blue arrow).

(B) Kidney tissues from male mice irradiated with 7.0 Gy, 1-month post-TBI, show fibrosis (asterisk) centered on the arcuate artery.

(C) Liver tissues representing all groups of female mice at 1-month post-TBI display a small focus of mononuclear cells with fewer neutrophils (solid arrow); also present are a few necrotic hepatocytes characterized by the loss of nuclei and hyper-eosinophilicity (open arrow).

(D) Lung tissues from a female mouse irradiated with 7.0 Gy, 6 months post-TBI, show broad sheets of lymphocytes.

(*Z* score = 2.449) compared to the non-irradiated male mice group (Figure 5A). However, the analysis revealed that other pathways were neither significantly activated (*Z* score ≥ 2) nor inhibited (*Z* score ≤ -2) in both the irradiated male and female mice groups at both time points, although in the R7.5_F1 group the HOTAIR regulatory pathway showed an inclination towards activation (*Z* score <2 i.e., 1.633) compared to the non-irradiated female mice group. Further, the canonical pathway "epithelial-mesenchymal transition by growth factors" also showed an inclination towards activation (*Z* score <2 i.e., 1) for both R7.5_M1 and R7.5_F1 groups compared to non-irradiated male and female mice groups, respectively (Figure 5A).

Conversely, analyses revealed that both pathways showed an inclination towards inhibition (*Z* score > −2) in the R7.5_M6 and R7.5_F6 groups compared to non-irradiated male and female mice, respectively. The *Z* score for the HOTAIR regulatory pathway was −0.816 for both R7.5_M6 and R7.5_F6 groups, and for the epithelial-mesenchymal transition by growth factors was −1 for both R7.5_M6 and R7.5_F6 groups. Figure 5B shows the legend for the bubble bot, where the colors indicate the *Z* score and the sizes of the bubbles indicate the number of overlapping genes. As depicted in Figures 5C–5F, the HOTAIR regulatory pathway was analyzed as a member of the cellular growth, proliferation and development, and cancer category. The regulation of the epithelial-mesenchymal transition by growth factors was analyzed as a member of the organismal growth and development and growth factor signaling category (Figures 5C–5F). Collectively, these results reveal that in response to DEARE the regulation of the HOTAIR canonical pathway varies in a time- and sex-dependent manner in the murine serum of the irradiated male and female mice groups.

Regulation of upstream signaling molecules varies in a time- and sex-dependent manner

The large variations in the expression of miRNAs in response to DEARE, at both post-TBI time points and pathways involved in cellular and organismal growth and development, as well as cancer, urged to examine the potential master regulator genes that would have the role as key modulators in response to DEARE. To investigate this, we performed IPA upstream regulator analysis for differentially expressed miRNAs in the serum of the irradiated male and female mice groups at both post-TBI time points. The analysis identified that several transcriptional upstream regulators were either activated or inhibited in response to DEARE at months 1 and 6 post-TBI, in both sexes. The activation (+*Z* score) and inhibition (-Z score) of upstream regulators and the expression of associated miRNAs in the serum from the irradiated male and female mice groups at 1 and 6 months post-TBI compared to non-irradiated male and female mice groups, respectively, are shown in Tables S3 and S4.

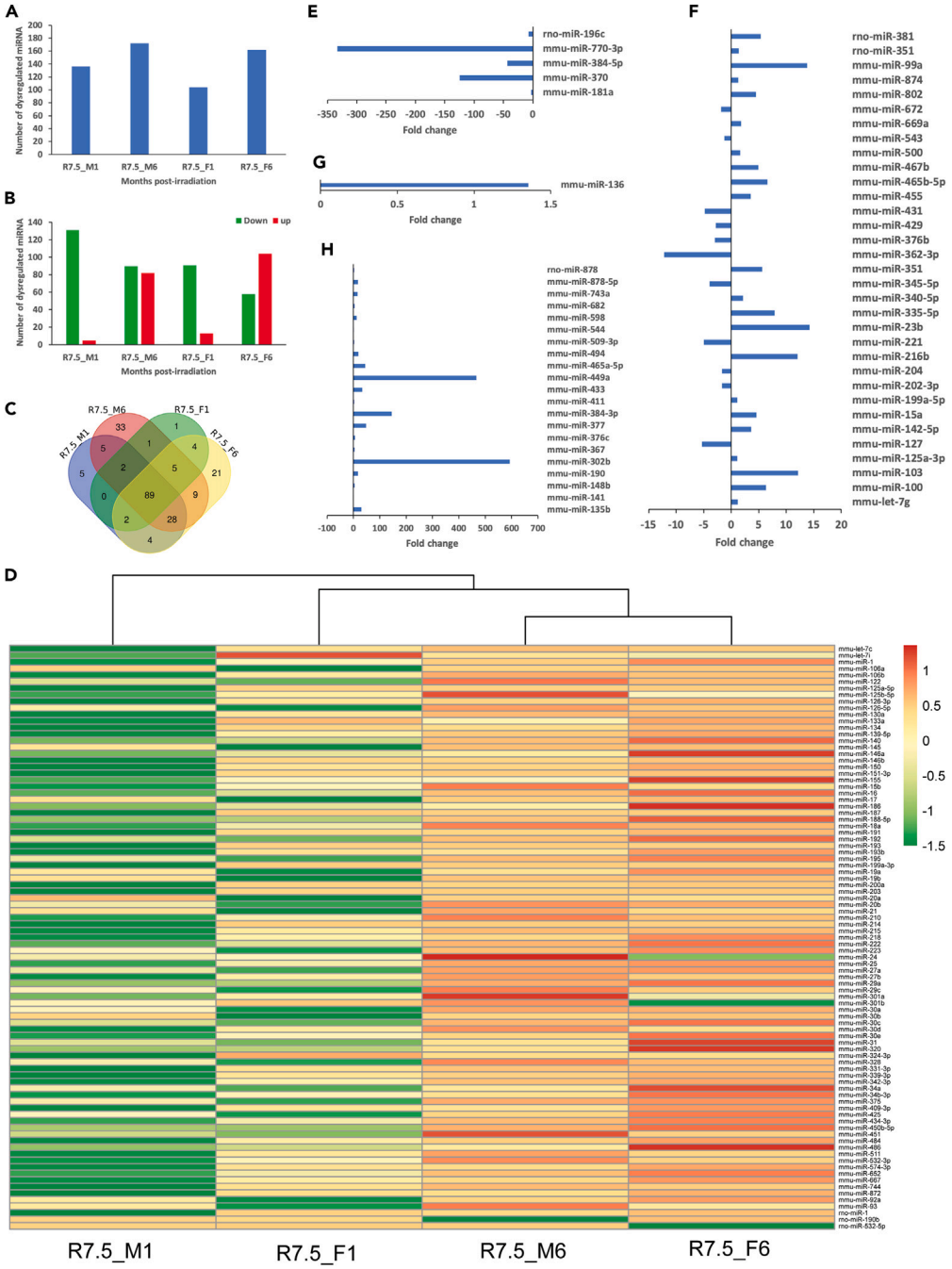

Figure 4. Differentially expressed miRNAs

The histogram displays (A) the total number of dysregulated miRNAs, (B) including both downregulated and upregulated miRNAs; (C) the Venn diagram illustrates the total number of miRNAs expressed commonly and specifically; (D) the heatmap demonstrates the expression of commonly dysregulated miRNAs in serum samples of irradiated male and female mice, compared to their respective age-matched non-irradiated control groups. The bar graph shows the expression of time- and sex-specific miRNAs in the following groups: (E) R7.5_M1, (F) R7.5_M6, (G) R7.5_F1, and (H) R7.5_F6, compared to their respective age-matched non-irradiated control groups.

Activation or inhibition of upstream regulator in R7.5_M1 and R7.5_M6

Interestingly, in R7.5_M1 group, compared to non-irradiated male group, the analysis showed that the regulatory molecules such as insulin, Gnasas1, follicle-stimulating hormone (FSH), DNA-methyltransferase, and c-Src were significantly activated (Z score ≥ 2), and the regulators involved in miRNA biogenesis (such as AGO1, AGO2, DGCR8, and DICER1) and other regulators (such as single-strand DNA-binding

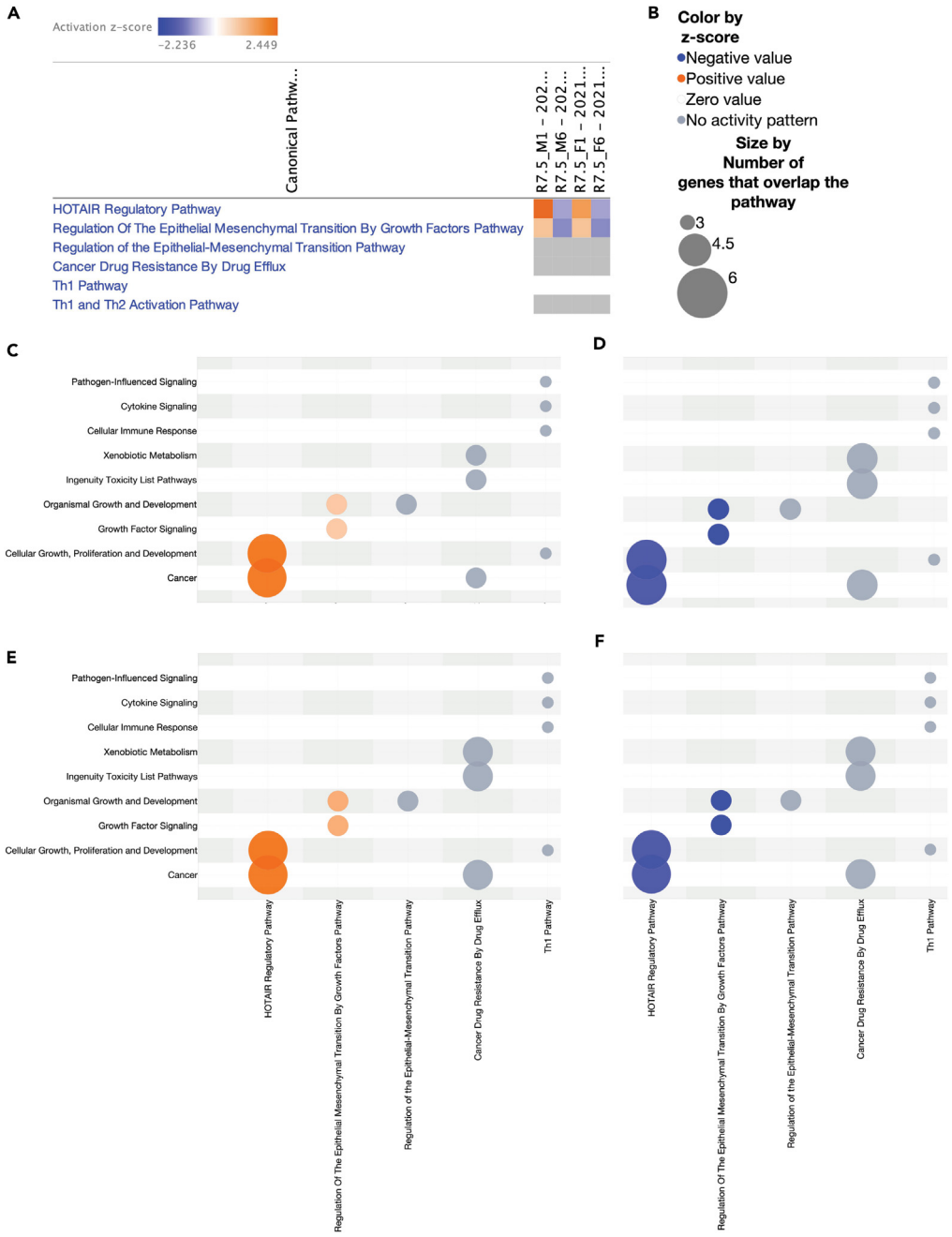

Figure 5. Differentially regulated canonical signal transduction pathways

(A) The heatmap shows the activation or inhibition of canonical signaling pathways in murine serum samples from the R7.5_M1, R7.5_M6, R7.5_F1, and R7.5_F6 groups, compared to their respective age-matched non-irradiated control groups.

(B) Legend for bubble chart: the colors indicate the *Z* score, and the sizes of the bubbles increase with the number of overlapping genes. Bubble chart displays the clustering of canonical pathways and their scores into categories in murine serum samples from (C) R7.5_M1, (D) R7.5_M6, (E) R7.5_F1, and (F) R7.5_F6 groups, compared to their respective age-matched non-irradiated control groups.

protein (SSB), E2F3, EPHB6, NF2, IGF1R, E2F1, E2F2, INSR, Smad2/3, LATS2, and PARN) were significantly inhibited (*Z* score ≤ -2) (Figure 6A), whereas, in R7.5_M6 group compared to non-irradiated male group, the analysis revealed that none of the regulatory molecules were significantly activated (*Z* score ≥ 2) or inhibited (*Z* score ≤ -2). Although some regulators involved in miRNA biogenesis (such as AGO1, AGO2, DGCR8, DICER1, and DROSHA) and other regulators (such as insulin, Gnasas1, FSH, DNA-methyltransferase, c-Src, RE1-silencing transcription factor (REST), E2F3, EPHB6, NF2, IGF1R, INSR, and PARN) indicated inclination towards inhibition (*Z* score > -2), such as SSB, E2F1, E2F2,

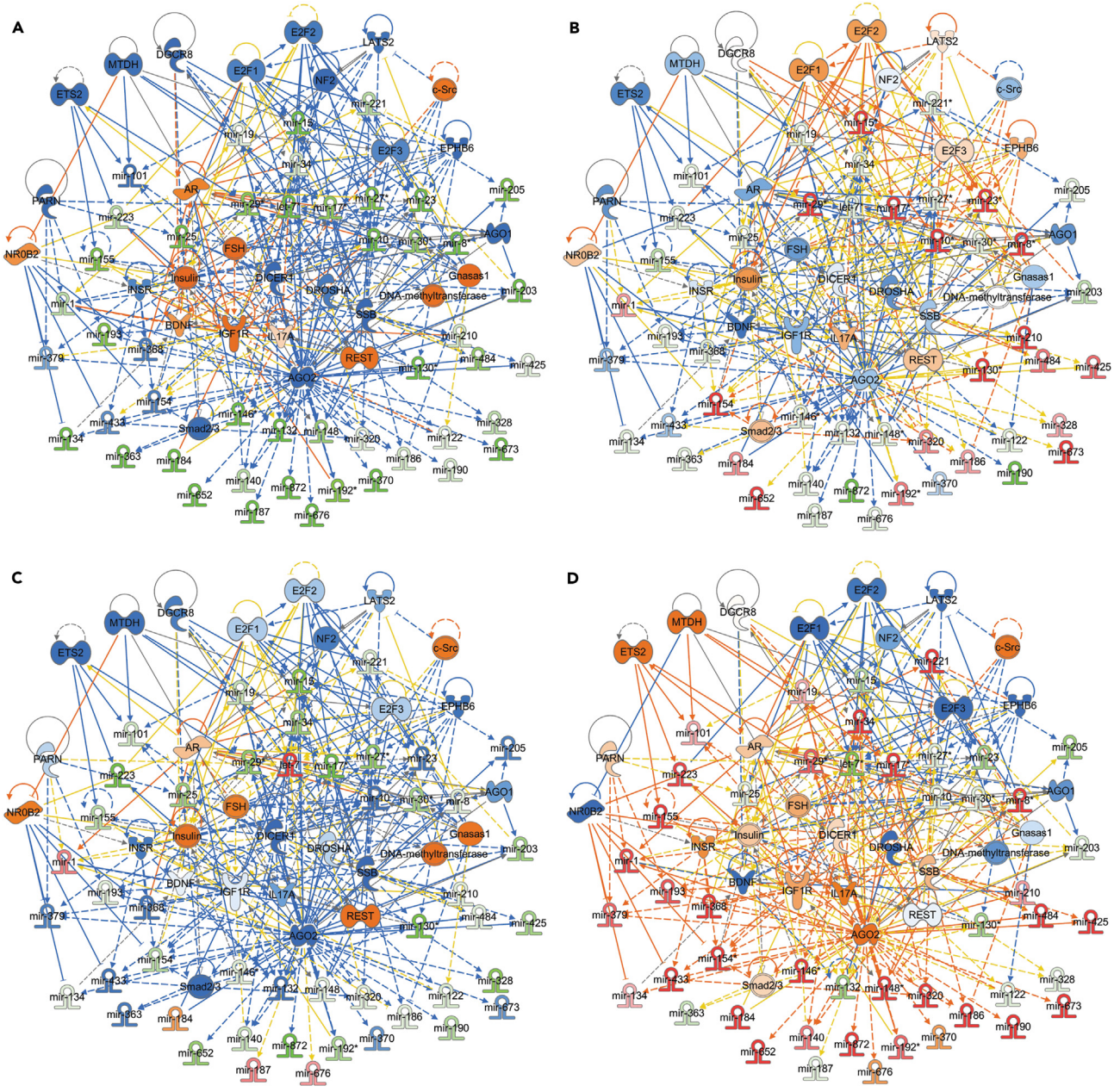

Figure 6. Differentially regulated upstream signaling molecules and associated miRNAs

Upstream regulators analyzed to be activated or inhibited in murine serum samples from (A) R7.5_M1, (B) R7.5_M6, (C) R7.5_F1, and (D) R7.5_F6, in comparison to their respective age-matched non-irradiated control groups. The color scheme indicates the value of the differential expressions, while the shapes represent the type and function, as indicated in Figure S2. Solid arrows represent genes that interact directly, and dotted arrows represent indirect interactions between genes.

Smad2/3, and LATS2 indicated inclination towards activation (*Z* score <2) (Figure 6B). Together, these results suggest that in response to DEARE activation or inhibition of upstream signaling molecules is time dependent in the serum of irradiated male mice.

Activation or inhibition of upstream regulator in R7.5_F1 and R7.5_F6

The analysis of the R7.5_F1 group, compared to the non-irradiated female group, showed that regulatory molecules such as insulin, Gnasas1, DNA-methyltransferase, and REST were significantly activated (*Z* score ≥ 2). In addition, regulators involved in miRNA biogenesis (such as AGO2 and DICER1) and other regulators (such as SSB and Smad2/3) were significantly inhibited (*Z* score ≤ -2) (Figure 6C). On the other hand, in the R7.5_F6 group, compared to the non-irradiated female group, the analysis indicated significant activation (*Z* score ≥ 2) of

IL17A and AGO2, and significant inhibition (Z score ≤ -2) of DROSHA, NROB2, and Brain-derived neurotrophic factor (BDNF) (Figure 6D). Although other regulatory molecules in the R7.5_F6 group were not significantly activated (Z score ≥ 2) or inhibited (Z score ≤ -2), there was a tendency towards inhibition (Z score > -2) of insulin, Gnasas1, DNA-methyltransferase, REST, DICER1, and SSB, and a tendency towards activation (Z score <2) of Smad2/3 in this group. These results suggest that in response to DEARE activation or inhibition of upstream signaling molecules is time dependent in the serum of irradiated female mice.

Activation or inhibition of upstream regulators between male and female mice

Furthermore, the analysis showed that after one-month post-TBI, in response to DEARE, the R7.5_M1 group exhibited significant activation (Z score ≥ 2) of FSH and significant inhibition of regulators related to miRNA biogenesis (AGO1, DGCR8) and other regulators (E2F3, EPHB6, NF2, IGF1R, E2F1, E2F2, INSR, LATS2, PARN). In contrast, R7.5_F1 showed no significant activation (Z score ≥ 2) or inhibition (Z score ≤ -2) for these regulatory molecules but exhibited a trend toward FSH activation and the inhibition of miRNA biogenesis regulators (AGO1, DGCR8, E2F3, EPHB6, NF2, IGF1R, E2F1, E2F2, INSR, LATS2, PARN) (Figures 6A and 6B). Similarly, after six months post-TBI, in response to DEARE, the R7.5_F6 group of mice exhibited significant activation (Z score ≥ 2) of AGO2 and IL17A, while DROSHA, NROB2, and BDNF were significantly inhibited (Z score ≤ -2) (Figure 6D). In contrast, the R7.5_M6 group showed no significant activation (Z score ≥ 2) or inhibition (Z score ≤ -2) for these regulatory molecules but indicated a tendency towards AGO2, DROSHA, and BDNF inhibition (Z score > -2) and IL17A and NROB2 activation (Z score <2) (Figure 6C). These findings underscore the time- and sex-dependent nature of the activation or inhibition of upstream signaling molecules in response to DEARE.

Regulation of disease and cellular function varies in a time- and sex-dependent manner

Subsequently, to distinguish the cellular processes and biological functions involved with DEARE, we performed IPA disease and cellular function analysis with the differentially expressed miRNAs in the serum of the irradiated male and female mice groups at both post-TBI time points compared to non-irradiated male and female mice, respectively. The analysis identified that at months 1 and 6 in response to DEARE several molecular patterns associated with a (patho)physiological process were either activated or inhibited in both sexes.

Commonly dysregulated disease and cellular functions

The analysis revealed that in response to DEARE certain molecular patterns associated with a (patho)physiological process were commonly activated or inhibited in both sexes and at all time points (R7.5_M1, R7.5_M6, R7.5_F1, and R7.5_F6), as shown in Figures S3A–S3D. These activated functions included G1/S phase transition of embryonic cell lines, interphase of embryonic cell lines, invasive tumor, maturation of chondrocyte cell lines, and migration of hepatoma cell lines. Inhibited functions included liver metastasis and secondary neoplasm of the digestive system. These results suggest that the activation or inhibition of several molecular patterns associated with a (patho)physiological process in response to DEARE is independent of time and sex in the serum of irradiated male and female mice at months one and six.

Time-dependent dysregulation of disease and cellular functions

Our findings show that in response to DEARE certain molecular patterns associated with a (patho)physiological process were activated or inhibited in R7.5_M1 and R7.5_F1. These activated functions included cell movement of tumor cell lines, expression of RNA, migration of tumor cell lines,Protein kinase B (PKB) signaling, quantity of cells, and transcription. On the other hand, differentiation of muscle cell lines and proliferation of epithelial cell lines were inhibited. This is depicted in Figures S4A and S4C. In R7.5_M6 and R7.5_F6, the functional activities of these disease cellular functions were reversed, as shown in Figures S4B and S4D. These outcomes suggest that the activation or inhibition of several molecular patterns associated with a (patho)physiological process in response to DEARE is time dependent and independent of sex in the serum of irradiated male and female mice at months one and six.

Time- and sex-dependent dysregulation of disease and cellular functions

Furthermore, intriguingly, we found that in response to DEARE some molecular patterns associated with a (patho)physiological process were particularly dysregulated in either R7.5_M6 or R7.5_F6, while being dysregulated in a reverse manner in all other murine serum samples, as depicted Figures 7A–7D. For example, in R7.5_M6 some molecular patterns associated with a (patho)physiological process were either activated (such as apoptosis of hepatoma cell lines, apoptosis of tumor cell lines, and cell death of tumor cell lines) or inhibited (such as cell proliferation of hepatoma cell lines and growth of solid tumor) (Figure 7B), while functional activities of these molecular patterns were reversed in all other murine serum samples. Similarly, the results showed that in R7.5_F6 some molecular patterns associated with a (patho)physiological process were either activated (such as hematopoiesis of mononuclear leukocytes) or inhibited (such as cytokinesis of ventricular myocytes, development of cardiovascular tissue, development of epithelial tissue, endothelial cell development, migration of breast cancer cell lines, neoplasia of carcinoma cell lines, proliferation of rhabdomyosarcoma cell lines, proliferation of vascular cells, sprouting angiogenesis, and vasculogenesis) (Figure 7D), while functional activities of these molecular patterns were reversed in all other murine serum samples. These outcomes suggest that in response to DEARE activation or inhibition of several molecular patterns associated with a (patho)physiological process is time and sex dependent in the serum of irradiated male and female mice at months one and six.

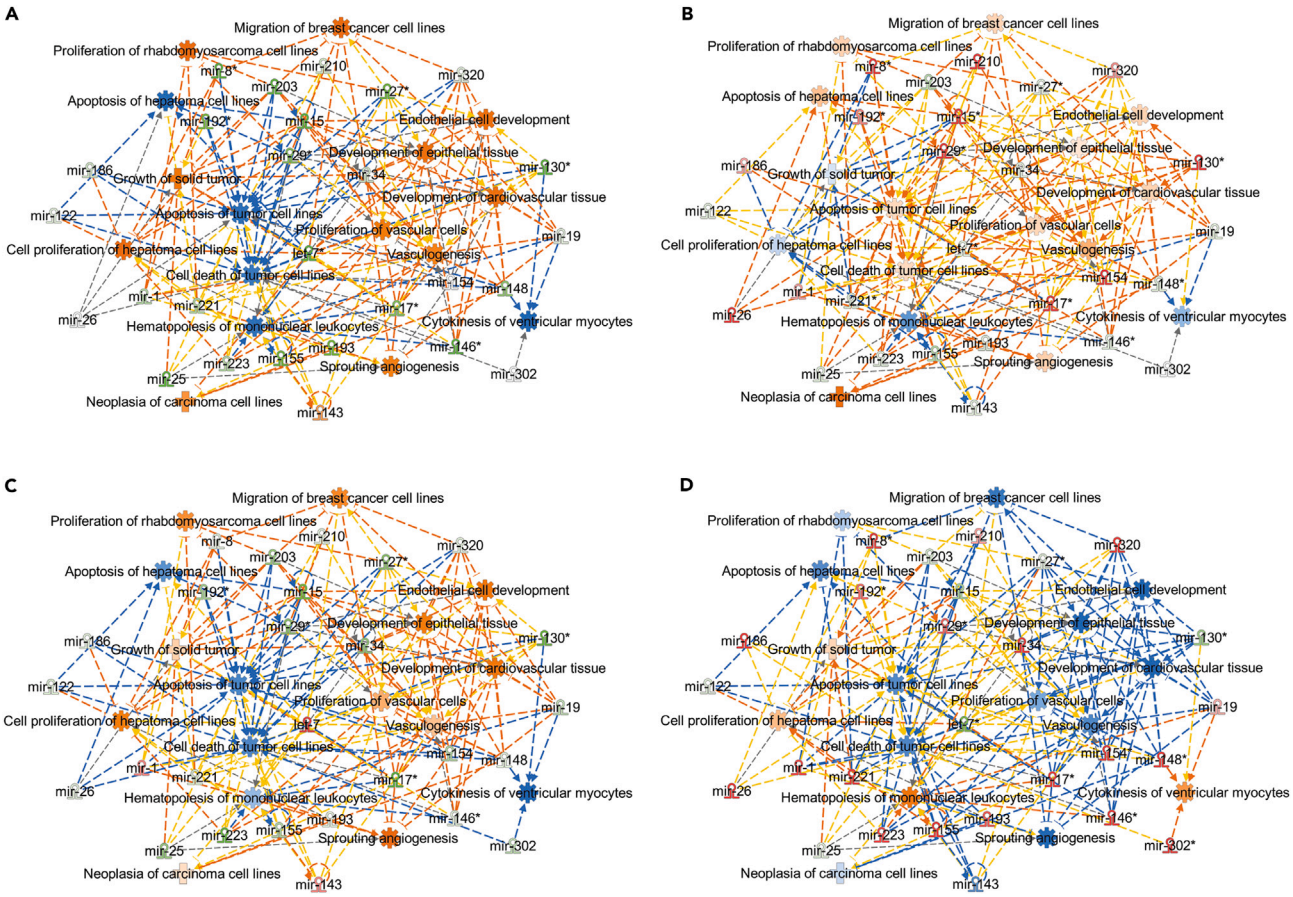

Figure 7. Time- and sex-dependent dysregulation of disease and cellular functions

Molecular patterns associated with a (patho)physiological process analyzed to be time and sex dependent activated or inhibited in murine serum samples from (A) R7.5_M1, (B) R7.5_M6, (C) R7.5_F1, and (D) R7.5_F6, compared to their respective age-matched non-irradiated control groups. The color scheme indicates the value of the differential expressions, while the shapes represent the type and function, as indicated in Figure S2. Solid arrows represent direct gene interactions, and dotted arrows represent indirect interactions between genes.

DISCUSSION

The DEARE can include chronic illnesses in multiple organs and serious health problems such as cancer, cardiovascular disease, and hereditary issues. Factors such as radiation dose, exposure duration, radiation quality, age, sex, and the health of the exposed individual can influence the severity of DEARE. Previous research has documented various disparities between the sexes in the incidence of thyroid cancer, lung cancer, breast cancer, prostate cancer, blood-based ailments, and reproductive system-related disorders among those who survived the Chernobyl nuclear reactor disaster, atomic bomb exposure, and occupational exposure to ionizing radiation.[9,11,31,32] However, the detailed understanding of sex-specific differences in the long-term response to radiation exposure is limited. Further research is needed to gain a better understanding of the sex-specific differences and the cellular and molecular mechanisms that contribute to the varying degrees of DEARE in males and females, to inform medical interventions, treatments, and radiation safety guidelines.

Mouse models have proven successful in supporting epidemiological findings in biological studies. These models enable analyses to be conducted under standardized conditions and can yield conclusive evidence regarding the proposed sex-specific radiation sensitivity.[18–26,33] In this study, we performed a robust 30-day animal studies with 6 escalating radiation doses (7–9 Gy) and find that females are more radioresistant than males. Probit analysis of the lethal dose curves shows that LD50/30 is 7.76 Gy for male mice and 8.08 Gy for female mice. In addition, we demonstrate here that at 6 months post-TBI (both 7.5 and 8 Gy) increased survivors in female mice were found compared to male mice. Recently, work from our lab analyzing survival curves in male and female mice from various studies demonstrated a slight yet statically significant increase in female mice survival compared to male mice survival, a trend which was also observed in the current work.[34] It is expected that mice manifest DEARE including abnormalities and pathological changes in major tissues and organs as long-term effect following radiation exposure. While comparing BW increases over 6 months post-TBI in male vs. female mice, BW gain was similar in both sexes. We also did not observe major sex differences in blood cell parameters, bone marrow progenitor cells, or megakaryocyte numbers in bone marrow sternum. Histopathological analysis of both male and female mice demonstrated

abnormalities in random animals in all irradiated groups at 1 and 6 months post-TBI in liver, kidney, heart, and lungs except no abnormalities found with heart in 6 months post-TBI group.

The cellular reactions to radiation are intricate and involve a multitude of sex-specific molecular processes. These include alterations in gene expression, initiation of signal transduction chains through DNA damage or conformational changes in receptors on the membrane, repair mechanisms that remove or tolerate DNA damage, cell proliferation, and responses like cell-cycle arrest and apoptosis.[18,20,21,35–41] Essentially, differences in sex-specific physiological mechanisms such as hormonal factors, viral infections, and lifestyle, could lead to a sex-specific response to radiation in the entire organism, including disparities in these molecular processes. Therefore, to understand the effect of DEARE in radioresistance in 6 months post-TBI surviving mice, we compared miRNA profile in male vs. female mice. We have chosen 7.5 Gy dose to compare the genomic profile since higher number of survivors were found with female mice compared to male mice at 6 months post-TBI.

MiRNAs, which are short RNAs that do not code for proteins, play a role in regulating almost all cellular processes, such as DNA repair, apoptosis, necrosis, cell-cycle arrest, and survival. Under typical circumstances, the expression of miRNAs is meticulously controlled through various mechanisms, including genetic or epigenetic changes, recruitment of transcription factors, and the proper functioning of the effectors involved in miRNA production.[42,43] Any disruption to these mechanisms can lead to alterations in miRNA expression. Exposure to radiation can disturb numerous cellular processes, such as DNA repair, apoptosis, necrosis, cell-cycle arrest, and survival.[44] To counteract these cellular responses, the cell can initiate various modifications, including alterations in miRNA expression that vary depending on the dose, time, and tissue type.[22,45–50] Our current analyses show that in response to DEARE expression of miRNA varies in a time- and sex-dependent manner in the murine serum. In comparison to non-irradiated male and female groups, miRNA profiling of serum samples from irradiated male and female groups revealed 136 and 172 dysregulated miRNAs at one and 6 months post-TBI, respectively, and 104 and 162 dysregulated miRNAs, likewise. Additionally, discrepancies in expression pattern and levels were observed among miRNAs altered in all 4 groups R7.5_M1, R7.5_M6, R7.5_F1, and R7.5_F6, with 5, 33, 1, and 21 miRNAs specific to R7.5_M1, R7.5_M6, R7.5_F1, and R7.5_F6 groups, respectively. In corroboration, Koturbash et al. reported time- and sex-specific changes in miRNA expression in brain tissue of male and female mice exposed to TBI.[51] Similarly, the sex-specific alteration in the expression of miRNAs in spleen and thymus tissue has been revealed in mice exposed to TBI.[22] Further, several other studies report time-dependent alteration in miRNA expression in serum, plasma, and whole blood of mice exposed to TBI.[46–49] Along with available literature, our outcomes suggest that in response to DEARE upregulation or downregulation of miRNA is time and sex dependent in the serum of irradiated male and female mice at months one and six post-TBI.

The observed significant differences in the miRNA expression between male and female mice at different time intervals indicate the possibility of identifying potential sex-specific master regulator genes that play a crucial role as key modulators in the sex-based development of diseases induced by radiation. In our upstream regulator analysis for differentially expressed miRNAs in the irradiated male and female mice groups, we find that in response to DEARE at one-month post-TBI enzymes of miRNA processing such as AGO1 and DGCR8 are significantly inhibited in the irradiated male mice group. Conversely, our results demonstrate only an inclination towards inhibition in the irradiated female mice group. Furthermore, at six-month post-TBI, the analysis shows that in response to DEARE enzymes of miRNA processing such as AGO2 and DROSHA are significantly activated and inhibited, respectively, in the irradiated female mice group, while only an inclination towards inhibition was observed in the irradiated male mice group. According to prior research, inhibition of miRNA biogenesis—achieved by suppressing miRNA processing enzymes AGO2 or DICER in endothelial cells—was found to enhance cell death following irradiation.[52] The expression of DROSHA and DICER was observed to be lower in radiosensitive cell lines compared to resistant ones.[53] A recent study has proposed that miRNA biogenesis, or some of its processing enzymes, may be directly regulated by radiation.[48] Together, our results suggest a response to DEARE in the form of activation or inhibition of upstream signaling molecules (including miRNA processing enzymes) and thereby dysregulation of miRNA expression and biogenesis is time and sex dependent. This is a new and unexplored field of research, as the interplay between different members of the miRNA production pathway and their response to radiation is still largely unknown. The potential for groundbreaking discoveries in this area is vast, as miRNAs hold great promise as regulators of cellular stress and the underlying mechanisms.

Subsequently, canonical pathway analysis identifies the HOTAIR regulatory pathway and epithelial-mesenchymal transition by growth factors as the affected pathways in response to DEARE in the serum samples of the irradiated male and female mice groups. Intriguingly, our results show that regulation of the HOTAIR canonical pathway varies in a time- and sex-dependent manner. Further analysis shows that the HOTAIR regulatory pathway is a member of the cellular growth, proliferation and development, and cancer category. The regulation of the epithelial-mesenchymal transition by growth factors is a member of the organismal growth and development and growth factor signaling category. Earlier, the association between the long noncoding RNAs (lncRNA) HOTAIR and radiosensitivity/radioresistance has been documented in various studies. For instance, overexpression of HOTAIR increased the radioresistance of pancreatic ductal adenocarcinoma cells, cervical cancer cell lines, and HeLa and C33A cells by modulating WIF-1, HIF-1α, and p21, respectively.[54–56] In addition, knockdown of HOTAIR in breast cancer cell lines resulted in increased radiosensitivity, DNA damage, and cell-cycle arrest due to the suppression of miR-218.[57] Additionally, the role of HOTAIR in the regulation of cellular radiosensitivity was reported via the sponging of miR-449b-5p in breast cancer cell lines.[58] Along with previous reports, our data suggest that radiation-induced dysregulation of HOTAIR regulatory pathway has a prominent impact on radiosensitivity in response to DEARE in a time- and sex-dependent manner.

The exposure to radiation can cause disruptions in various cellular processes, such as cell growth, death, invasion, metastasis, genomic stability, energy metabolism, inflammation, and immune response.[59,60] Consistently, we also conducted an analysis of disease and cellular functions using miRNAs that showed differential expression in the serum samples of both male and female groups at one and six months

after exposure. The analysis shows that in response to DEARE several cellular functions are commonly, irrespective of time and sex, dysregulated in the irradiated male and female mice at months one and six. For instance, G1/S phase transition of embryonic cell lines, interphase of embryonic cell lines, invasive tumor, maturation of chondrocyte cell lines, and migration of hepatoma cell lines are activated at both post-TBI time points and in both sexes. Similarly, liver metastasis and secondary neoplasm of digestive system are inhibited at both post-TBI time points and in both sexes.

Further, we also find that in response to DEARE activation or inhibition of several molecular patterns associated with a (patho)physiological process is time and sex dependent in the serum of irradiated male and female mice at months one and six post-TBI. The notable contrast in functional control mechanisms between male and female mice strongly indicates the importance of developing sex-specific targets for immune or apoptosis-based radioprotectors and mitigators. The observed significant differences in the miRNA expression, upstream regulators, and canonical pathways following radiation exposure, among both male and female mice at different time intervals, represent a significant and innovative discovery that may provide a plausible explanation for the sex-based development of diseases induced by radiation.

In summary, the findings indicate that female mice display higher survival rates and resistance to radiation compared to male mice at 6 months following TBI. DEARE triggers a dysregulation in the expression and biogenesis of miRNA in a time- and sex-specific manner, leading to the irregularity of molecular and cellular mechanisms, which have varying effects on male and female disease functions. In general, the results show that DEARE impacts males and females differently and at different times, which calls for significant alterations to radiation safety protocols. Further preclinical studies are requisite to fully comprehend the time- and sex-specific mechanism of DEARE and to devise an effective therapeutic approach to prevent DEARE in humans.

Limitations of the study

The current study does provide a time-resolved analysis of DEARE in both sexes of C57BL/6 mice; however, there are limitations to the study. In particular, the study utilized animals which survived lethal doses of radiation exposure; this resulted in relatively low animal numbers, particularly as the dose of radiation increased. More broadly, this study utilized the C57BL/6 strain. This strain is widely used in radiation research; however, other strains such as C3H/HeN are more radiosensitive and CD2F1 are more radioresistant. Conducting similar analyses in these strains would serve to demonstrate the conserved nature of the alterations identified here. Finally, as with all radiation research this work is done in animal models in an attempt to predict the human response; conducting analyses in additional species would provide additional insight into conserved changes which may predict the human response.

STAR★METHODS

Detailed methods are provided in the online version of this paper and include the following:

- KEY RESOURCES TABLE
- RESOURCE AVAILABILITY
  - Lead contact
  - Materials availability
  - Data and code availability
- METHOD DETAILS
  - Use of male and female mice
  - Irradiation conditions and dosimetry
  - Ethics statement
  - Veterinary care following radiation
  - Blood and tissue collection
  - Hematopoietic progenitor clonogenic assay
  - Histopathology
  - Total RNA extraction
  - Murine microRNA analysis
  - Pathway analyses
- QUANTIFICATION AND STATISTICAL ANALYSIS

SUPPLEMENTAL INFORMATION

Supplemental information can be found online at https://doi.org/10.1016/j.isci.2024.108867.

ACKNOWLEDGMENTS

The authors gratefully acknowledge Bernadette Hritzo and Zemenu Aschenake for technical assistance. The authors wish to thank the board-certified pathologists Dr. Jerrold M. Ward and Dr. Sang H. Lee for histopathological analysis. Support for the work was provided by grants from the National Institute of Allergy and Infectious Diseases (AA112044-001-04000 to S.P.G.) and the AFRRI Intramural funding

RAB21093220. The opinions contained herein are the personal views of the authors and are not necessarily those of Armed Forces Radiobiology Research Institute, the Uniformed Services University of the Health Sciences, or the Department of Defense.

AUTHOR CONTRIBUTIONS

S.B., V.P.K., G.P.H.-H., K.W., and S.P.G. conducted experiments. V.P.K., G.P.H.-H., and S.P.G. designed experiments. D.K.S., S.B., R.B., V.P.K., G.P.H.-H., and K.W. analyzed the data. D.K.S., G.P.H.-H., R.B., and S.P.G. wrote the manuscript.

DECLARATION OF INTERESTS

The authors declare no competing interests.

Received: June 21, 2023
Revised: September 28, 2023
Accepted: January 8, 2024
Published: January 11, 2024

REFERENCES

1. Institute of Medicine (US) Committee on Battlefield Radiation Exposure Criteria (1999). In Potential Radiation Exposure in Military Operations: Protecting the Soldier Before, During, and After, S. Thaul and H. O'Maonaigh, eds.
2. Van Moore, A., Jr. (2004). Radiological and nuclear terrorism: are you prepared? J. Am. Coll. Radiol. *1*, 54–58.
3. Christodouleas, J.P., Forrest, R.D., Ainsley, C.G., Tochner, Z., Hahn, S.M., and Glatstein, E. (2011). Short-term and long-term health risks of nuclear-power-plant accidents. N. Engl. J. Med. *364*, 2334–2341.
4. Gale, R.P., and Armitage, J.O. (2018). Are We Prepared for Nuclear Terrorism? N. Engl. J. Med. *378*, 2449–2450.
5. (2018). Acute Radiation Syndrome (ARS): A Fact Sheet for the Public. https://www.cdc.gov/nceh/radiation/emergencies/ars.htm.
6. Nakachi, K., Hayashi, T., Hamatani, K., Eguchi, H., and Kusunoki, Y. (2008). Sixty years of follow-up of Hiroshima and Nagasaki survivors: current progress in molecular epidemiology studies. Mutat. Res. *659*, 109–117.
7. Hsu, W.L., Tatsukawa, Y., Neriishi, K., Yamada, M., Cologne, J., and Fujiwara, S. (2010). Longitudinal trends of total white blood cell and differential white blood cell counts of atomic bomb survivors. J. Radiat. Res. *51*, 431–439.
8. Krestinina, L.Y., Epifanova, S., Silkin, S., Mikryukova, L., Degteva, M., Shagina, N., and Akleyev, A. (2013). Chronic low-dose exposure in the Techa River Cohort: risk of mortality from circulatory diseases. Radiat. Environ. Biophys. *52*, 47–57.
9. Narendran, N., Luzhna, L., and Kovalchuk, O. (2019). Sex Difference of Radiation Response in Occupational and Accidental Exposure. Front. Genet. *10*, 260.
10. Blakely, E.A. (2000). Biological effects of cosmic radiation: deterministic and stochastic. Health Phys. *79*, 495–506.
11. Yablokov, A.V., Nesterenko, V.B., and Nesterenko, A.V. (2009). Chernobyl: Consequences of the Catastrophe for People and the Environment. Ann. N. Y. Acad. Sci. *1181*, 1–327. vii-xiii.
12. Hansson, S.O. (2009). Should we protect the most sensitive people? J. Radiol. Prot. *29*, 211–218.
13. (2007). The 2007 Recommendations of the International Commission on Radiological Protection. Ann. ICRP *37*, 1–332. ICRP publication 103.
14. Harrison, J.D., Balonov, M., Bochud, F., Martin, C.J., Menzel, H.G., Smith-Bindman, R., Ortiz-López, P., Simmonds, J.R., and Wakeford, R. (2021). The use of dose quantities in radiological protection: ICRP publication 147 Ann ICRP 50(1) 2021. J. Radiol. Prot. *41*, 410–422.
15. National Research Council (2006). Health Risks from Exposure to Low Levels of Ionizing Radiation: BEIR VII Phase 2.
16. UNSCEAR (2006). Report to the General Assembly with Scientific Annexes, Effects of Ionizing Radiation. Volume I Report and Annexes A and B *2008*.
17. Olson, M. (2011). Atomic Radiation Is More Harmful to Women (Originally published by Nuclear Information and Resource Service).
18. Kovalchuk, O., Ponton, A., Filkowski, J., and Kovalchuk, I. (2004). Dissimilar genome response to acute and chronic low-dose radiation in male and female mice. Mutat. Res. *550*, 59–72.
19. Kovalchuk, O., Burke, P., Besplug, J., Slovack, M., Filkowski, J., and Pogribny, I. (2004). Methylation changes in muscle and liver tissues of male and female mice exposed to acute and chronic low-dose X-ray-irradiation. Mutat. Res. *548*, 75–84.
20. Silasi, G., Diaz-Heijtz, R., Besplug, J., Rodriguez-Juarez, R., Titov, V., Kolb, B., and Kovalchuk, O. (2004). Selective brain responses to acute and chronic low-dose X-ray irradiation in males and females. Biochem. Biophys. Res. Commun. *325*, 1223–1235.
21. Pogribny, I., Raiche, J., Slovack, M., and Kovalchuk, O. (2004). Dose-dependence, sex- and tissue-specificity, and persistence of radiation-induced genomic DNA methylation changes. Biochem. Biophys. Res. Commun. *320*, 1253–1261.
22. Ilnytskyy, Y., Zemp, F.J., Koturbash, I., and Kovalchuk, O. (2008). Altered microRNA expression patterns in irradiated hematopoietic tissues suggest a sex-specific protective mechanism. Biochem. Biophys. Res. Commun. *377*, 41–45.
23. Koturbash, I., Kutanzi, K., Hendrickson, K., Rodriguez-Juarez, R., Kogosov, D., and Kovalchuk, O. (2008). Radiation-induced bystander effects *in vivo* are sex specific. Mutat. Res. *642*, 28–36.
24. Unthank, J.L., Miller, S.J., Quickery, A.K., Ferguson, E.L., Wang, M., Sampson, C.H., Chua, H.L., DiStasi, M.R., Feng, H., Fisher, A., et al. (2015). Delayed Effects of Acute Radiation Exposure in a Murine Model of the H-ARS: Multiple-Organ Injury Consequent to <10 Gy Total Body Irradiation. Health Phys. *109*, 511–521.
25. Sharma, N.K., Holmes-Hampton, G.P., Kumar, V.P., Biswas, S., Wuddie, K., Stone, S., Aschenake, Z., Wilkins, W.L., Fam, C.M., Cox, G.N., and Ghosh, S.P. (2020). Delayed effects of acute whole body lethal radiation exposure in mice pre-treated with BBT-059. Sci. Rep. *10*, 6825.
26. Gasperetti, T., Miller, T., Gao, F., Narayanan, J., Jacobs, E.R., Szabo, A., Cox, G.N., Orschell, C.M., Fish, B.L., and Medhora, M. (2021). Polypharmacy to Mitigate Acute and Delayed Radiation Syndromes. Front. Pharmacol. *12*, 634477.
27. Guerra-Assunção, J.A., and Enright, A.J. (2012). Large-scale analysis of microRNA evolution. BMC Genom. *13*, 218.
28. Djuranovic, S., Nahvi, A., and Green, R. (2012). miRNA-mediated gene silencing by translational repression followed by mRNA deadenylation and decay. Science *336*, 237–240.
29. Bartel, D.P. (2004). MicroRNAs: genomics, biogenesis, mechanism, and function. Cell *116*, 281–297.
30. O'Connell, K.E., Mikkola, A.M., Stepanek, A.M., Vernet, A., Hall, C.D., Sun, C.C., Yildirim, E., Staropoli, J.F., Lee, J.T., and Brown, D.E. (2015). Practical murine hematopathology: a comparative review and implications for research. Comp. Med. *65*, 96–113.
31. Sokolnikov, M.E., Gilbert, E.S., Preston, D.L., Ron, E., Shilnikova, N.S., Khokhryakov, V.V., Vasilenko, E.K., and Koshurnikova, N.A. (2008). Lung, liver and bone cancer mortality in Mayak workers. Int. J. Cancer *123*, 905–911.
32. Biegon, A., Cohen, S., and Franceschi, D. (2022). Modulation of Secondary Cancer Risks from Radiation Exposure by Sex, Age and Gonadal Hormone Status: Progress, Opportunities and Challenges. J. Pers. Med. *12*, 725.
33. Medhora, M., Gao, F., Gasperetti, T., Narayanan, J., Khan, A.H., Jacobs, E.R., and

Fish, B.L. (2019). Delayed Effects of Acute Radiation Exposure (Deare) in Juvenile and Old Rats: Mitigation by Lisinopril. Health Phys. *116*, 529–545.

34. Holmes-Hampton, G.P., Kumar, V.P., Valenzia, K., and Ghosh, S.P. (2023). Sex as a factor in murine radiation research: implications for countermeasure development. Cytogenet. Genome Res. 1–10. https://doi.org/10.1159/000531630.
35. Cassie, S., Koturbash, I., Hudson, D., Baker, M., Ilnytskyy, Y., Rodriguez-Juarez, R., Weber, E., and Kovalchuk, O. (2006). Novel retinoblastoma binding protein RBBP9 modulates sex-specific radiation responses *in vivo*. Carcinogenesis *27*, 465–474.
36. Meadows, S.K., Dressman, H.K., Muramoto, G.G., Himburg, H., Salter, A., Wei, Z., Ginsburg, G.S., Chao, N.J., Nevins, J.R., and Chute, J.P. (2008). Gene expression signatures of radiation response are specific, durable and accurate in mice and humans. PLoS One *3*, e1912.
37. Rodemann, H.P., Dittmann, K., and Toulany, M. (2007). Radiation-induced EGFR-signaling and control of DNA-damage repair. Int. J. Radiat. Biol. *83*, 781–791.
38. Thomas-Ahner, J.M., Wulff, B.C., Tober, K.L., Kusewitt, D.F., Riggenbach, J.A., and Oberyszyn, T.M. (2007). Gender differences in UVB-induced skin carcinogenesis, inflammation, and DNA damage. Cancer Res. *67*, 3468–3474.
39. Schmitz, A., Bayer, J., Déchamps, N., and Thomas, G. (2003). Intrinsic susceptibility to radiation-induced apoptosis of human lymphocyte subpopulations. Int. J. Radiat. Oncol. Biol. Phys. *57*, 769–778.
40. Whitney, A.R., Diehn, M., Popper, S.J., Alizadeh, A.A., Boldrick, J.C., Relman, D.A., and Brown, P.O. (2003). Individuality and variation in gene expression patterns in human blood. Proc. Natl. Acad. Sci. USA *100*, 1896–1901.
41. Besplug, J., Burke, P., Ponton, A., Filkowski, J., Titov, V., Kovalchuk, I., and Kovalchuk, O. (2005). Sex and tissue-specific differences in low-dose radiation-induced oncogenic signaling. Int. J. Radiat. Biol. *81*, 157–168.
42. Croce, C.M. (2009). Causes and consequences of microRNA dysregulation in cancer. Nat. Rev. Genet. *10*, 704–714.
43. Iorio, M.V., and Croce, C.M. (2012). Causes and consequences of microRNA dysregulation. Cancer J. *18*, 215–222.
44. Adjemian, S., Oltean, T., Martens, S., Wiernicki, B., Goossens, V., Vanden Berghe, T., Cappe, B., Ladik, M., Riquet, F.B., Heyndrickx, L., et al. (2020). Ionizing radiation results in a mixture of cellular outcomes including mitotic catastrophe, senescence, methuosis, and iron-dependent cell death. Cell Death Dis. *11*, 1003.
45. Acharya, S.S., Fendler, W., Watson, J., Hamilton, A., Pan, Y., Gaudiano, E., Moskwa, P., Bhanja, P., Saha, S., Guha, C., et al. (2015). Serum microRNAs are early indicators of survival after radiation-induced hematopoietic injury. Sci. Transl. Med. *7*, 287ra69.
46. Cui, W., Ma, J., Wang, Y., and Biswal, S. (2011). Plasma miRNA as biomarkers for assessment of total-body radiation exposure dosimetry. PLoS One *6*, e22988.
47. Templin, T., Amundson, S.A., Brenner, D.J., and Smilenov, L.B. (2011). Whole mouse blood microRNA as biomarkers for exposure to gamma-rays and (56)Fe ion. Int. J. Radiat. Biol. *87*, 653–662.
48. Aryankalayil, M.J., Chopra, S., Makinde, A., Eke, I., Levin, J., Shankavaram, U., MacMillan, L., Vanpouille-Box, C., Demaria, S., and Coleman, C.N. (2018). Microarray analysis of miRNA expression profiles following whole body irradiation in a mouse model. Biomarkers *23*, 689–703.
49. Chakraborty, N., Gautam, A., Holmes-Hampton, G.P., Kumar, V.P., Biswas, S., Kumar, R., Hamad, D., Dimitrov, G., Olabisi, A.O., Hammamieh, R., and Ghosh, S.P. (2020). microRNA and Metabolite Signatures Linked to Early Consequences of Lethal Radiation. Sci. Rep. *10*, 5424.
50. Liang, X., Zheng, S., Cui, J., Yu, D., Yang, G., Zhou, L., Wang, B., Cai, L., and Li, W. (2018). Alterations of MicroRNA Expression in the Liver, Heart, and Testis of Mice Upon Exposure to Repeated Low-Dose Radiation. Dose Response *16*, 1559325818799561.
51. Koturbash, I., Zemp, F., Kolb, B., and Kovalchuk, O. (2011). Sex-specific radiation-induced microRNAome responses in the hippocampus, cerebellum and frontal cortex in a mouse model. Mutat. Res. *722*, 114–118.
52. Kraemer, A., Anastasov, N., Angermeier, M., Winkler, K., Atkinson, M.J., and Moertl, S. (2011). MicroRNA-mediated processes are essential for the cellular radiation response. Radiat. Res. *176*, 575–586.
53. Surova, O., Akbar, N.S., and Zhivotovsky, B. (2012). Knock-down of core proteins regulating microRNA biogenesis has no effect on sensitivity of lung cancer cells to ionizing radiation. PLoS One *7*, e33134.
54. Jing, L., Yuan, W., Ruofan, D., Jinjin, Y., and Haifeng, Q. (2015). HOTAIR enhanced aggressive biological behaviors and induced radio-resistance via inhibiting p21 in cervical cancer. Tumour Biol. *36*, 3611–3619.
55. Li, N., Meng, D.D., Gao, L., Xu, Y., Liu, P.J., Tian, Y.W., Yi, Z.Y., Zhang, Y., Tie, X.J., and Xu, Z.Q. (2018). Overexpression of HOTAIR leads to radioresistance of human cervical cancer via promoting HIF-1alpha expression. Radiat. Oncol. *13*, 210.
56. Jiang, Y., Li, Z., Zheng, S., Chen, H., Zhao, X., Gao, W., Bi, Z., You, K., Wang, Y., Li, W., et al. (2016). The long non-coding RNA HOTAIR affects the radiosensitivity of pancreatic ductal adenocarcinoma by regulating the expression of Wnt inhibitory factor 1. Tumour Biol. *37*, 3957–3967.
57. Hu, X., Ding, D., Zhang, J., and Cui, J. (2019). Knockdown of lncRNA HOTAIR sensitizes breast cancer cells to ionizing radiation through activating miR-218. Biosci. Rep. *39*, BSR20181038.
58. Zhang, S., Wang, B., Xiao, H., Dong, J., Li, Y., Zhu, C., Jin, Y., Li, H., Cui, M., and Fan, S. (2020). LncRNA HOTAIR enhances breast cancer radioresistance through facilitating HSPA1A expression via sequestering miR-449b-5p. Thorac. Cancer *11*, 1801–1816.
59. Lewanski, C.R., and Gullick, W.J. (2001). Radiotherapy and cellular signalling. Lancet Oncol. *2*, 366–370.
60. Wang, J.S., Wang, H.J., and Qian, H.L. (2018). Biological effects of radiation on cancer cells. Mil. Med. Res. *5*, 20.
61. Kumar, V.P., Holmes-Hampton, G.P., Biswas, S., Stone, S., Sharma, N.K., Hritzo, B., Guilfoyle, M., Eichenbaum, G., Guha, C., and Ghosh, S.P. (2022). Mitigation of total body irradiation-induced mortality and hematopoietic injury of mice by a thrombopoietin mimetic (JNJ-26366821). Sci. Rep. *12*, 3485.
62. Ghosh, S.P., Pathak, R., Kumar, P., Biswas, S., Bhattacharyya, S., Kumar, V.P., Hauer-Jensen, M., and Biswas, R. (2016). Gamma-Tocotrienol Modulates Radiation-Induced MicroRNA Expression in Mouse Spleen. Radiat. Res. *185*, 485–495.
63. Satyamitra, M., Kumar, V.P., Biswas, S., Cary, L., Dickson, L., Venkataraman, S., and Ghosh, S.P. (2017). Impact of Abbreviated Filgrastim Schedule on Survival and Hematopoietic Recovery after Irradiation in Four Mouse Strains with Different Radiosensitivity. Radiat. Res. *187*, 659–671.
64. Soni, D.K., Kumar, V.P., Biswas, S., Holmes-Hampton, G.P., Bhattacharyya, S., Thomas, L.J., Biswas, R., and Ghosh, S.P. (2022). CDX-301 prevents radiation-induced dysregulation of miRNA expression and biogenesis. Mol. Ther. Nucleic Acids *30*, 569–584.
65. Metsalu, T., and Vilo, J. (2015). ClustVis: a web tool for visualizing clustering of multivariate data using Principal Component Analysis and heatmap. Nucleic Acids Res. *43*, W566–W570.

STAR★METHODS

KEY RESOURCES TABLE

REAGENT or RESOURCE	SOURCE	IDENTIFIER
Experimental models: Organisms/strains		
Mice	Jackson Laboratories	C57BL/6J
Mouse feed	Harlan Teklad	Rodent Diet 8604
Chemicals, peptides, and recombinant proteins		
CBC Diluent	Heska	CAT 5222
CBC Diff Lyse	Heska	CAT 5223
LH Lyse	Heska	CAT 5225
Probe Cleanser	Heska	CAT 5228
Pre-Surgical Panel E-Wrap	Heska	CAT 6330-PRESURG/EWRAP
AST (GOT)	Heska	CAT 6330-AST
Methocult GF+ system for mouse cells	StemCell Technologies	M3434
Critical commercial assays		
mirVana PARIS RNA purification kit	Thermo Fisher	AM1556
TaqMan MicroRNA Reverse Transcription Kit	Thermo Fisher	4366596
Megaplex PreAmp Primers	Thermo Fisher	4399203
TaqMan Universal PCR Master Mix, No AmpErase UNG	Thermo Fisher	4352042
TaqMan™ Rodent MicroRNA A Array v2.0	Thermo Fisher	4398967
Software and algorithms		
Expression Suite Software V1.0.3	Thermo Fisher	https://apps.thermofisher.com/apps/spa/#/dashboard
Venn diagram	Bioinformatics & Evolutionary Genomics	https://bioinformatics.psb.ugent.be/webtools/Venn/
Clustvis	Clustvis: a web tool for visualizing clustering of multivariate data (BETA)	https://biit.cs.ut.ee/clustvis/
Ingenuity Pathway Analyses (IPA)	QIAGEN Inc	https://digitalinsights.qiagen.com/IPA
GraphPad Prism	GraphPad by Dotmatics	Version 9
SPSS	IBM SPSS Statistics	Version 25.0

RESOURCE AVAILABILITY

Lead contact

Further information and requests for resources and reagents should be directed to Sanchita P. Ghosh (Sanchita.ghosh@usuhs.edu).

Materials availability

This study did not generate new reagents.

Data and code availability

- The datasets generated during and/or analyzed during the current study are available from the corresponding author on reasonable request.
- This paper does not report original code.
- Any additional information required to reanalyze the data reported in this paper is available from the lead contact upon request.

METHOD DETAILS

Use of male and female mice

Pathogen free male and female C57BL/6 male and female mice (12-14 weeks old) were purchased from Jackson Laboratories (Bar Harbor, ME). Animals were housed as reported previously[61] in the Uniformed Services University of the Health Sciences (USUHS) Department of Laboratory Animal Resources (DLAR) facility and acclimated for a minimum of 5 days prior to use in experiments. Animals were identified by tail tattoos. Both room and cage humidity were maintained between 30% - 70% and 10-15 air changes/hour occurred in housing room. An automated lighting system was used providing a 12-hour light, 12-hour dark cycle. Mice were provided Harlan Teklad Global Rodent Diet 8604 *ad libitum* from the feeder rack within the cage. During critical periods of peak mortality, food pellets were added directly to the floor of the cage in addition to being distributed from the feeder rack. This is a means of providing ease of access to animals that might struggle to obtain the food otherwise. Water was made available to animals *ad libitum* from bottles attached to individual cages. The water provided is acidified pH~2.5 from an Edstrom water bottle filling station. All procedures pertaining to animals were reviewed and approved by the USUHS Institutional Animal Care and Use Committee (IACUC) using the principles outlined in the National Research Council's Guide for the Care and Use of Laboratory Animals and performed in accordance with relevant guidelines and regulations.

Animal studies were conducted in compliance with ARRIVE (Animal Research: Reporting of *In Vivo* Experiments) guidelines. Handling of the animals was conducted in accordance with the USUHS IACUC and included the use of personal protective equipment (e.g. hair bonnets, facemasks, lab coat, gloves, and shoe covers). Animals were handled inside a fume hood with a HEPA (high efficiency particulate air) filtration system. During tissue collection in formalin buffer, appropriate PPE and fume hood/ventilation was used. Animals were weighed and randomly assigned into different groups based on the study design. Veterinary care was available throughout the course of the study, animals were examined by the veterinary staff as well as laboratory staffs as warranted by clinical signs or changes in appearance.

Irradiation conditions and dosimetry

For irradiation, the animals were transported in a climate-controlled van to the Armed Forces Radiobiology Research Institute (AFRRI) facility. After animals were received at the AFRRI, they were rested for a minimum of 60 min prior to irradiation in custom made Lucite restrained boxes with 8 compartments. After radiation exposure, animals were returned to their cages and ultimately returned to the DLAR facility via the climate-controlled van.

Mice were irradiated bilaterally (simultaneously) at an estimated dose rate of 0.6 Gy/min in the Cobalt-60 gamma-irradiation facility at AFRRI. Both males and female mice were irradiated at six doses at a dose rate of ~0.6 Gy/min from non-lethal to ~95% lethal doses (7 to 8.5 Gy). An alanine/Electron Spin Resonance (ESR) dosimetry system (American Society for Testing and Material Standard E 1607) has been used to measure the dose rates in the cores of acrylic phantoms (3 inches long and 1 inch in diameter) placed in all empty slots of the Lucite boxes. ESR signals were measured with a calibration curve based on standard calibration dosimeters provided by the National Institute of Standard and Technology (NIST, Gaithersburg, MD). The calibration curve was verified by inter-comparison with the National Physical Laboratory (NPL) in the United Kingdom. The corrections applied to the measured dose rates in phantoms were for decay of the Co-60 source and for a small difference in mass-energy absorption coefficients for water and soft tissue at the Co-60 energy level. The radiation field was previously reported to be uniform within $\pm$2%.[62]

Ethics statement

This study was conducted under an animal use protocol approved by the USUHS IACUC Protocol Number: AFR-20-999 following USDA Animal Welfare Act (21 CFR Part 9), and Public Health Service Policy, the Guide for the Care and Use of Laboratory animals, and the Office of Laboratory Animal Welfare as applicable. The Testing Facility is accredited by the Association for the Assessment and Accreditation of Laboratory Animal Care (AAALAC) International.

Veterinary care following radiation

Since animals were irradiated from non-lethal to almost 95% lethal doses, they were monitored three to four times daily following exposure. Irradiated mice experience a critical period of peak mortality during ~8 to ~26 days depending on the dose level) when they start showing clinical symptoms of pain and distress including unresponsiveness, abnormal posture, unkempt appearance, immobility, and lack of coordination. Animals that were found dead in the course of the study were documented and removed from the cage. Mice were considered moribund when they showed an inability to remain upright, were cold, unresponsive or displayed decreased or labored respiration. Morbid animals were monitored very closely according to their health in accordance with pre-defined criteria described and approved in the IACUC protocol. Moribund mice were euthanized according to American Veterinary Medical Association (AVMA) guidelines. Animals were weighed prior to the start of the experiment, during the course of the study animals that have lost more than 35% of their initial body weight were euthanized.

Blood and tissue collection

Blood samples (~20uL) were obtained from the animals (n=5-8) through the submandibular vein at two different time points (1 and 6 months). These samples were utilized to obtain complete blood counts (CBC) using the Heska Element HT5 Veterinary Hematology Analyzer (Heska/Cuattro Loveland, CO). At the 1- and 6-month marks following exposure to radiation, blood was collected from the animals under anesthesia

(5% Isoflurane, Baxter International Inc., Deerfield, IL) for serum collection in BD microtainer tubes (Beckton, Dickinson and Company, Franklin Lakes, NJ). After leaving the samples to clot for 1 hour, they were separated via centrifugation at 2400xg for 10 minutes. The animals were euthanized after the blood collection was complete through cervical dislocation, and femurs, sterna, spleens, hearts, lungs, and kidneys were collected. Depending on the specific analysis to be conducted, these tissues were collected in 10% buffered formalin, 4% paraformaldehyde, or flash-frozen.

Hematopoietic progenitor clonogenic assay

The clonogenic potential of mouse bone marrow cells were assessed by measuring colony formation in semisolid cultures. To achieve this, 1 mL of Methocult GF+ system for mouse cells (Stem Cell Technologies Inc., Vancouver, BC) was used as per the manufacturer's guidelines and previously described methods.[25,63] Colony-forming units (CFUs) were counted from samples obtained at both 1 and 6 months. Bone marrow cells were obtained from the femurs of three different animals, washed twice with Iscove Modified Dulbecco Media, and seeded onto 35-cm cell culture dishes (BD Biosciences) at a concentration of 1 to 5 $\times 10^4$ cells per dish. All samples were plated in duplicate and incubated for 14 days before scoring. The Methocult GF+ system was used to identify and quantify granulocyte-erythrocyte-monocyte-macrophage CFUs (CFU-GEMM), burst-forming unit-erythroid (BFU-E), and colony-forming unit granulocyte-macrophage (CFU-GM) in accordance with the manufacturer's instructions. Colonies were counted using a Nikon TS100F microscope after 14 days, and the data were presented as mean $\pm$ standard error of mean.

Histopathology

Samples of liver, kidney, heart, and sternum were obtained for histological examination after 1 and 6 months. The tissues were preserved in a 10% buffered formalin solution for at least 24 hours. Decalcification of sternum was performed using 12-18% sodium EDTA (pH 7.4-7.5) for 3 hours. Prior to embedding in paraffin, all the tissues were dehydrated using graded ethanol ranging from 70% to 100%. Hematoxylin and eosin (H&E) staining was utilized to stain the sections, and images were captured using an Olympus BX41 camera and analyzed with Adobe Photoshop. A board-certified veterinary pathologist conducted a blinded histopathological examination of all the samples.

Total RNA extraction

The mirVana PARIS RNA purification kit (Life Technologies, Frederick, MD) was utilized to extract total RNA from serum. To evaluate the concentration and quality of the serum RNAs, a NanoDrop spectrophotometer (NanoDrop Technologies, Wilmington, DE, USA) was employed, and all RNA samples showed absorbance ratios of 1.8-2.0 at 260/280 nm.

Murine microRNA analysis

Standard methods published by the vendor and previously described[64] were employed to conduct miRNA analysis. TaqMan MicroRNA Reverse Transcription Kit from Applied Biosystems was used to perform multiplex reverse transcription. After reverse transcription, Megaplex PreAmp Primers and TaqMan Preamp Master Mix (2X) were used for pre-amplification. The PreAmp product was then utilized to prepare PCR Reaction Mix using TaqMan Universal PCR Master Mix, No AmpErase UNG (2x). To run the PCR, 100 μL of the RT reaction-specific PCR reaction mix was loaded into the corresponding fill ports of the TaqMan Low-Density Rodent MicroRNA Panel v2.0 and run on 7900HT Fast Real-time PCR System (Applied Biosystems) using default thermal-cycling conditions.

Data analysis was conducted using Expression Suite Software V1.0.3 (ThermoFisher Cloud, Applied Biosystems, ThermoFisher Scientific Inc., Waltham, MA, USA) to determine the relative fold changes of each miRNA at different time intervals in male (R7.5_M1 and R7.5_M6) and female (R7.5_F1 and R7.5_F6) mice that were irradiated, compared to age-matched non-irradiated mice. The comparative cycle threshold CT ($2^{-\Delta\Delta CT}$) method with global normalization was employed using the relative quantification (Rq) approach. Additionally, a comparison was made between the miRNAs that were significantly altered (at various time intervals) in the R7.5_M groups and those in the R7.5_F groups, and the Venn diagrams were generated using the online tool https://bioinformatics.psb.ugent.be/webtools/Venn/. Clustvis (https://biit.cs.ut.ee/clustvis/), a web tool that employs Principal Component Analysis and heatmap for visualizing clustering of multivariate data, was used to construct the heatmaps.[65]

Pathway analyses

We conducted an *in-silico* analysis on miRNAs that were differentially expressed in the serum of mice from different groups, with a fold change of more than 0.5 but less than 1.2. The analysis was done using Ingenuity Pathway Analyses (IPA) from QIAGEN Inc. (https://www.qiagenbioinformatics.com/products/ingenuity-pathway-analysis), which relied on both experimentally observed and highly predicted data from the Ingenuity Knowledge Base data sources. Our goal was to identify the top canonical pathways, significant regulators, diseases and functions, and gene networks that were relevant to our study. We categorized the differentially expressed genes according to their specific functions and used them to create functional networks between miRNAs, their target genes, and regulatory molecules.

QUANTIFICATION AND STATISTICAL ANALYSIS

Thirty day and 6 months survival data were plotted as Kaplan-Meier plots. GraphPad Prism 9 software was utilized to perform Fisher's exact test to compare survival at 30 days or 6 months post-radiation and a log-rank test to compare survival curves over the monitoring period.

Probit analysis was conducted to determine the lethal doses of male and female mice with IBM SPSS Statistics 25.0 and a student's t-test was used to assess differences between the groups. Averages were reported +/- standard error of the mean (SEM). Hematological parameters were graphed as means ± SEM. These data were analyzed by two-way ANOVA. A p value of <0.05 was considered significant. Student's t-test was used to determine a significant difference between two groups in evaluating body weight change.

The expression levels of miRNAs in each group at different time points were compared using a Student's t-test. Heatmaps were created by clustering the miRNA expression data using the Euclidean distance metric for similarity and the average linkage method for association. Fisher's Exact Test was employed to conduct pathway analyses on miRNAs that were differentially expressed between groups at various time points. A p-value of less than 0.05 was considered statistically significant.